Communications Research Centre

IONOSPHERIC EFFECTS ON THE DOPPLER FREQUENCY SHIFT IN SARSAT PROPAGATION

by

D.B. MULDREW AND H.G. JAMES

CRC REPORT NO. 1313

Department of Communications
Ministère des Communications

OTTAWA, FEBRUARY 1978

COMMUNICATIONS RESEARCH CENTRE

DEPARTMENT OF COMMUNICATIONS
CANADA

IONOSPHERIC EFFECTS ON THE DOPPLER FREQUENCY SHIFT IN SARSAT PROPAGATION

by

D.B. Muldrew and H.G. James

(Radio and Radar Research Branch)

CRC REPORT NO. 1313

February 1978
OTTAWA

TABLE OF CONTENTS

IONOSPHERIC EFFECTS ON THE DOPPLER FREQUENCY SHIFT IN SARSAT PROPAGATION

by

D.B. Muldrew and H.G. James

ABSTRACT

The Doppler frequency shift of signals propagating from an Emergency Locator Transmitter (ELT) on a downed aircraft up to a transponder on a search and rescue satellite (SARSAT) and down to a central station is affected by the ionosphere. In this report ionospheric effects are estimated for a proof-of-concept SARSAT experiment using the AMSAT OSCAR-6 satellite. In this case, the down link is at 30 MHz and the daytime ionosphere with no horizontal gradients in electron density can change the Doppler frequency by a few hertz. Horizontal gradients of electron density can have more effect on the Doppler frequency than the vertical distribution of density since the negative vertical density gradient in the topside ionosphere tends to compensate the Doppler effect due to the positive gradient in the bottomside. In the late afternoon, evening and nighttime, large east-west troughs in the density distribution exist which can produce shifts of a few tens of hertz at 30 MHz. The Doppler frequency shift due to the ionosphere varies approximately inversely as the frequency. The results obtained here can be applied to the definition of an operational SARSAT system.

1. INTRODUCTION

The Communications Research Centre is involved in a program called SARSAT (Search and Rescue Satellite) to locate downed aircraft. The program is funded by the Department of National Defence who have the responsibility for search and rescue in Canada.

By measuring the Doppler frequency shift of the signal from the aircraft's ELT (Emergency Locator Transmitter) after it has been received by a satellite and retransmitted on a different frequency to a central station [Lambert and Winter, 1977] the position of a downed aircraft can be located. Ignoring the effect of the ionosphere on the Doppler frequency will increase the error in estimating the location of the aircraft. This report examines the ionospheric effect in some detail.

The ionosphere has a small but significant effect on the Doppler frequency shift of a VHF signal propagating between a moving satellite and fixed ground station. The Doppler frequency shift, hereafter called "Doppler", is the same whether the signal travels from the satellite to the ground or vice versa. Although the 30 MHz OSCAR 6 signal is transmitted from the satellite and received on the ground, for convenience in the derivations of this report, it will be assumed that the signal is transmitted from the ground and received at the satellite. The Doppler is given by

$$f_D = - \frac{1}{2\pi} \underline{k} \cdot \underline{v} = - \frac{1}{2\pi} kv \cos\lambda \qquad (1.1)$$

where $\underline{k}$ is the wave normal at the satellite of a VHF signal transmitted from the ground station and arriving at the satellite moving with velocity $\underline{v}$ and λ is the angle between $\underline{k}$ and $\underline{v}$ at the satellite. For reception at the satellite, if $\underline{k}$ has a component in the direction $\underline{v}$, f_D is taken to be negative. For a satellite at a height well above the F2-layer peak, the ionospheric effect on λ only need be considered. Here only the Doppler between the satellite and fixed station is considered; in the SARSAT case the Doppler between the ELT and satellite must be added.

In this report the computer programs that have been developed to calculate the ionospheric effect on the Doppler are presented and discussed. Calculations based on specific ionospheric models are also presented.

2. DOPPLER FREQUENCY CALCULATIONS

The mathematics required for the Doppler frequency calculations is presented in Appendix I. A listing of the main program and most of the subroutines and a sample calculation (corresponding to the solid curve in Figure 8) are presented in Appendices II and III. A flow chart of the main program is presented here. The relation of the subroutines to the main program is given in the chart.

3. EXAMPLES OF IONOSPHERIC EFFECTS ON DOPPLER CURVES

3.1 DESCRIPTION OF MODEL

Doppler frequency shifts have been calculated for a variety of ionospheric density models and for three different OSCAR-6 orbits. One of the orbits passes almost vertically over the assumed 30 MHz ground receiver

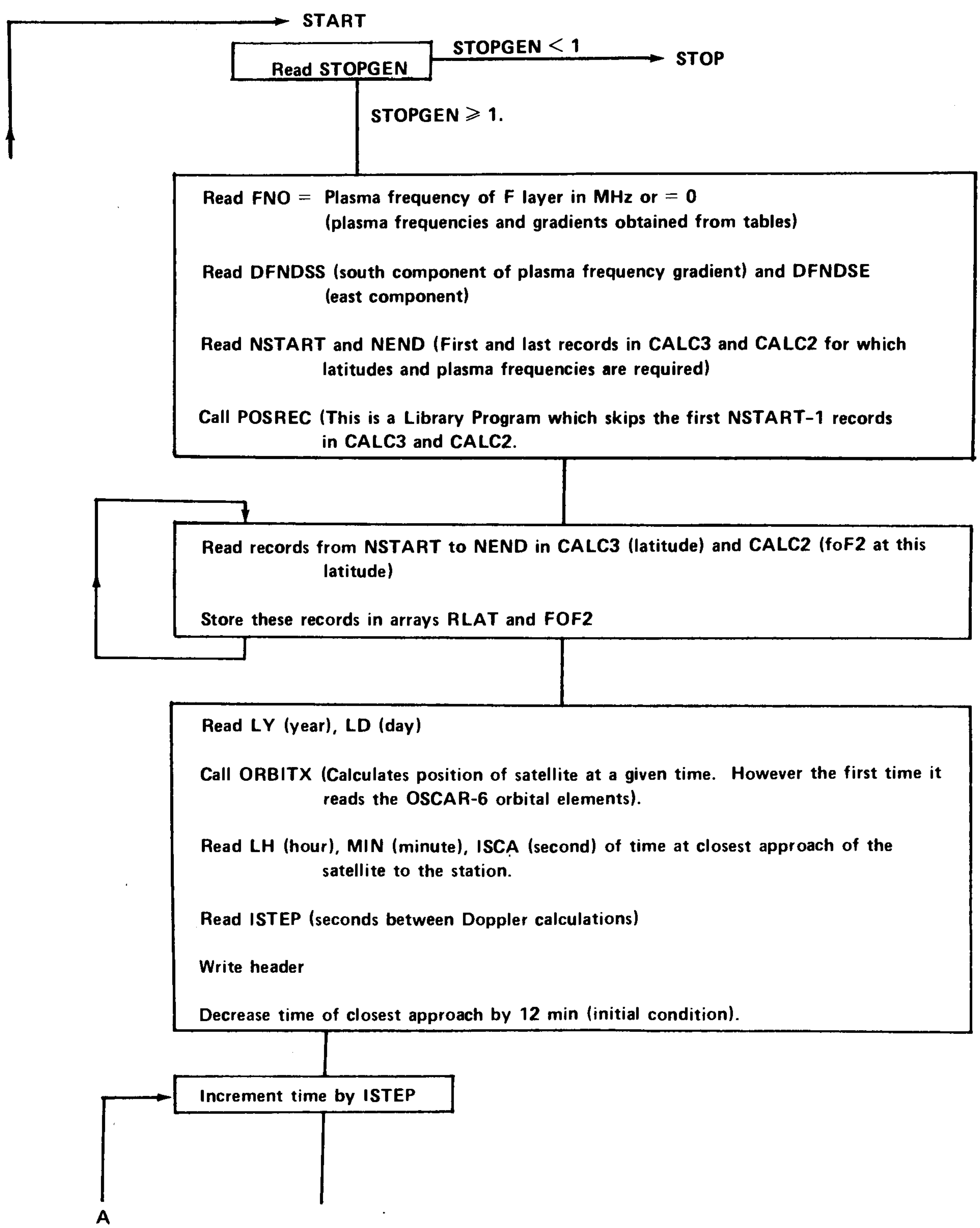

A Flow Chart of the Main Program (Sheet 1 of 3)

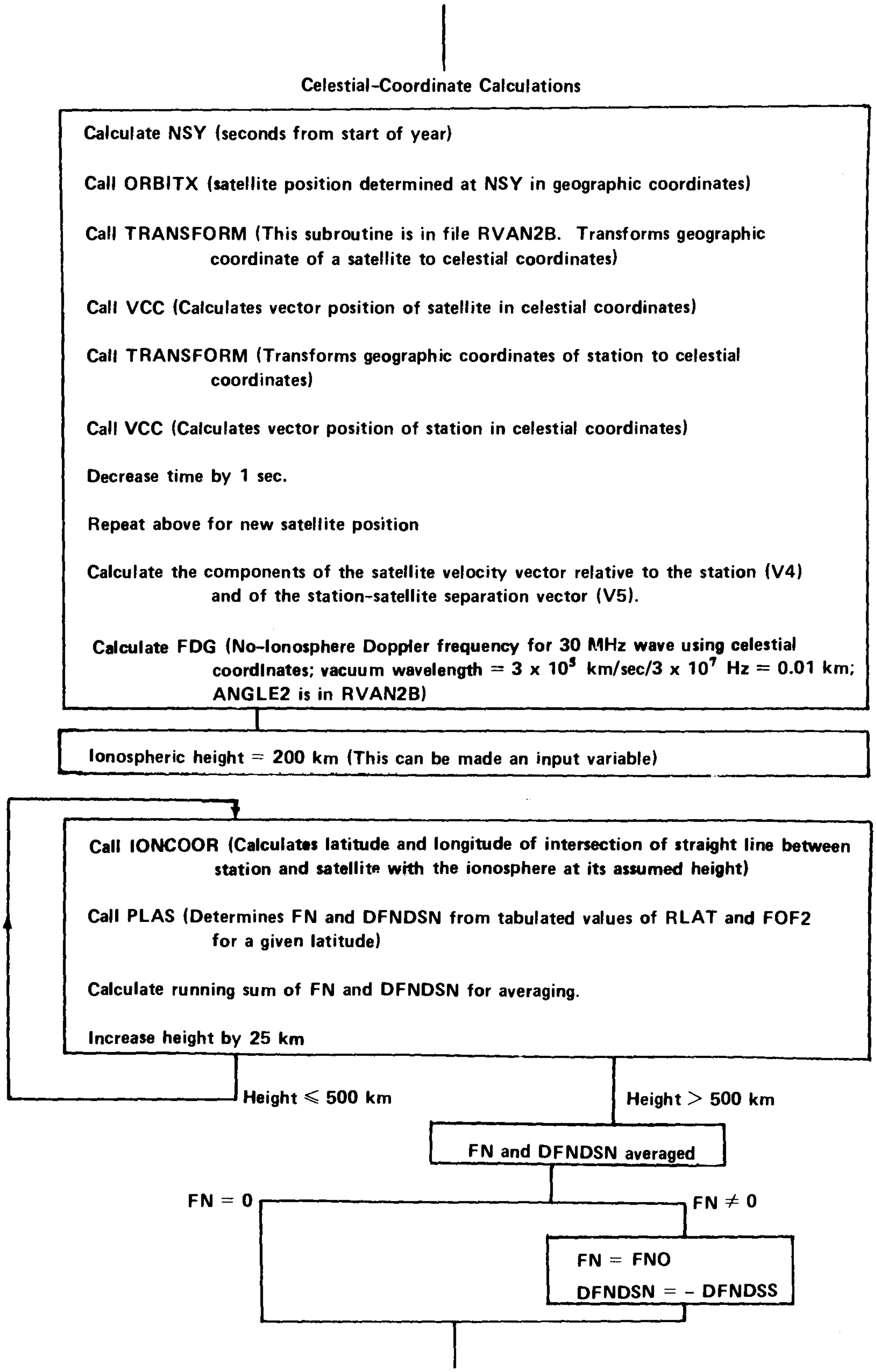

A Flow Chart of the Main Program (Sheet 2 of 3)

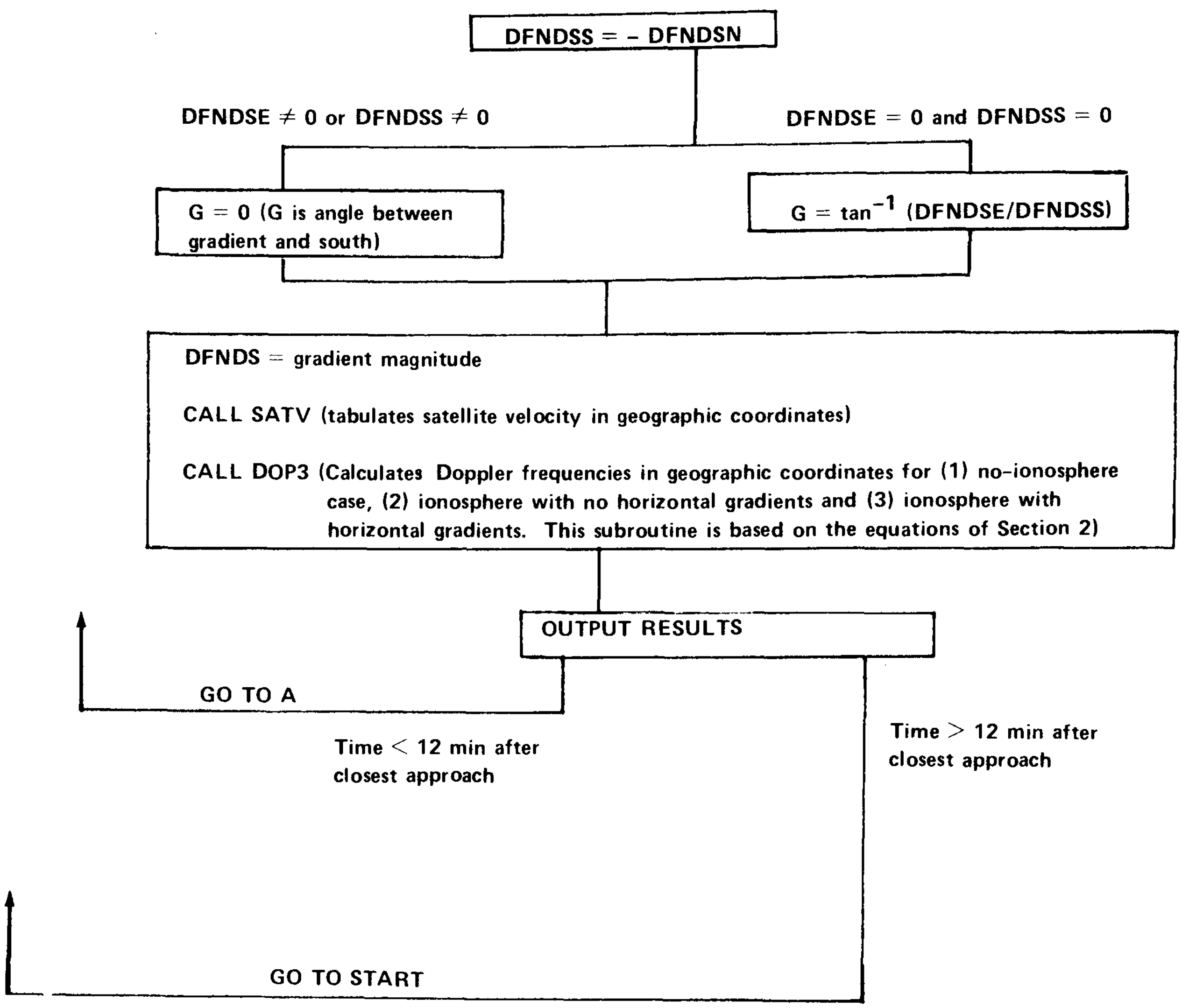

A Flow Chart of the Main Program (Sheet 3 of 3)

at Ottawa (45.36°N, 75.88°W) whereas the other two have subsatellite tracks that pass within about 2000 km of the receiver, one to the east and the other to the west. Ephemeris data for the passes were calculated on the CRC computer, using NASA-supplied Brouwer mean orbital elements for the spacecraft in conjunction with the ISIS orbit package. Various orbital details are given in Table 1.

TABLE 1

OSCAR–6 Passes Used in Study

Date	Time Interval Start	Stop	Closest GCD to Subsat. Point	Direction	Label
6 Jan/76	1620 UT	1644 UT	2280 km	Southbound	"West"
16 Jan/76	1403	1427	30	Southbound	"Overhead"
16 Jan/76	1210	1234	2240	Southbound	"East"

The tracks of the subsatellite points for the three passes, in relation to the location at Ottawa of the ground receiver are shown in Figure 1. OSCAR-6 is in a roughly circular orbit, and its height during these passes varies between 1448 and 1461 km. The orbit is retrograde with an inclination of approximately 110°, so that on these three north-to-south passes, the subsatellite track has a westward component of motion and makes an angle with the equator of about 70°. The first two lines in Table 1 correspond to passes during which CRC personnel carried out experimental ELT tests using a mobile transmitter and a receiver at Shirley Bay, whereas the "East" pass was not used for that purpose.

Ionospheric density distributions of various types have been modelled for the ray-tracing calculation of theoretical Doppler frequency shift on the satellite-to-ground 30 MHz signal. The ionosphere was approximated by a spherical layer 300 km thick lying between 200 and 500 km altitude. Within this layer the density could have horizontal gradients but no vertical gradients. In cases where the density varied along the ray path, the average density and horizontal gradient were obtained by averaging the values at each 25 km-height interval along the path. As explained in Appendix I, above 500 km and below 200 km altitude the waves propagate as in a vacuum and straight line rays are assumed.

Horizontal density gradients play an important role in determining ray paths and it was decided to include several values of density gradient in the Doppler calculations. The different models used are listed in Table 2. For Figure 2 a constant foF2 was used to evaluate the refractive index and a zero or east-west gradient was used to calculate the curvature of the ray path.

The difference in frequency between the Doppler shift, calculated with the ionosphere present and the free-space shift called the "ionospheric Doppler difference" is plotted as a function of the latitude of the OSCAR-6

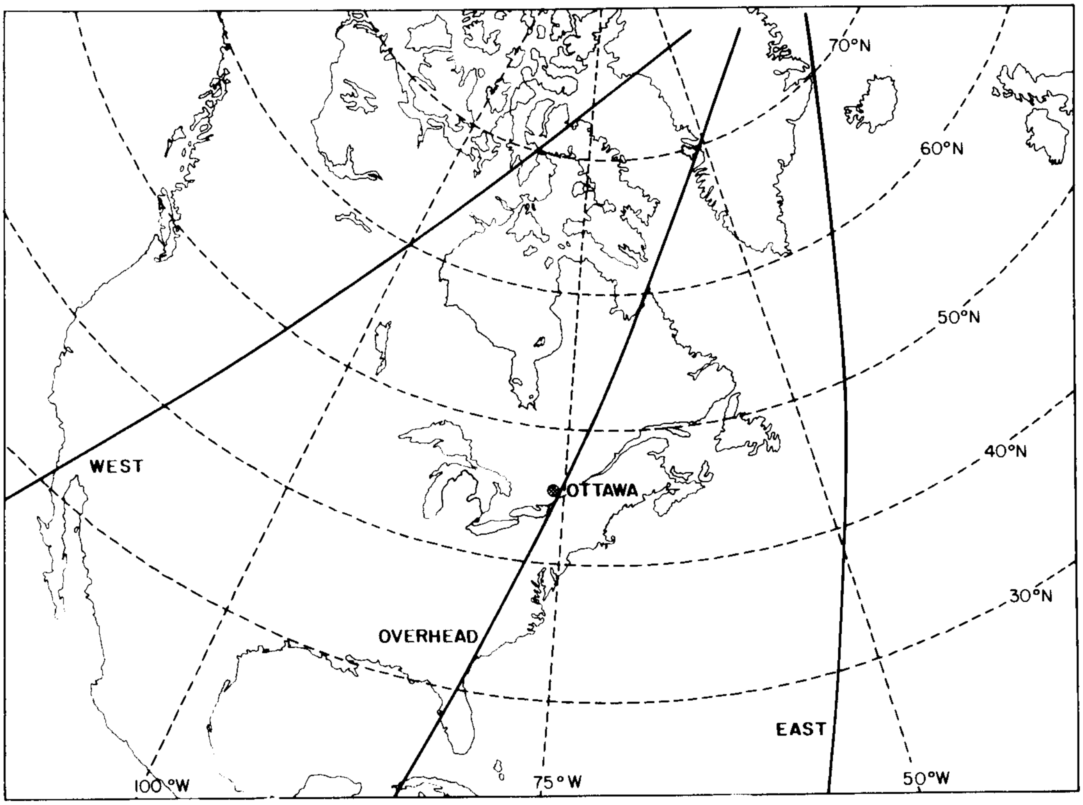

Figure 1. Subsatellite tracks of three OSCAR-6 passes, on a geographical coordinate frame

TABLE 2

Ionospheric Models

Figure No.	foF2	Horizontal Gradient in foF2	Comments
2	8 MHz	None, 0.001 MHz/km eastward, 0.001 MHz/km westward	
3	Varies	Varying north-south gradient	Both foF2 and gradient scaled from ionograms recorded on an Ottawa ISIS II pass starting 75/004/1442 UT.
4	Varies	Varying north-south gradient	Both foF2 and gradient scaled from ionograms recorded on an Ottawa ISIS II pass starting 75/009/1557 UT.
5a,b,c	Varies	Varying north-south gradient	Both foF2 and gradient derived from a hypothetical distribution composed of a deep ionospheric trough centred at Ottawa superposed on a constant southward gradient.
6	Varies	Varies	Constant eastward gradient of 0.0005 MHz/km is assumed. Both foF2 and north-south gradient are derived from ionograms recorded on an Ottawa ISIS II pass starting 75/003/1404 UT.

satellite (Figures 2 to 6). The difference frequency, although usually amounting to only several hertz in contrast to the total Doppler shift of a few hundreds of hertz, indicates the net effect of the ionosphere on the Doppler shift. The computer program starts calculating Doppler differences at 12 minutes before the instant of closest approach and proceeds at 50-second intervals through a 24-minute period. Near the beginning and the end of the pass, either the ionosphere reflects the rays or the satellite is out of range due to the earth's curvature and contact is no longer possible. The cutoff depends on the great circle separation of receiver and satellite and thus the latitude of cutoff is influenced by the longitude of the satellite. It will be seen that the low-latitude cutoff of the "west" pass is higher in latitude than that of the "east" pass.

3.2 RESULTS OF COMPUTATIONS

The models represent typical ionospheric conditions that a polar-orbiting SARSAT is likely to encounter. The cases are discussed in sequence:

3.2.1 Figure 2

The no-horizontal gradient case, corresponding to the dotted curves in Figure 2, obviously illustrates the importance of vertical gradients only, and provides a baseline for comparison with the later cases. At high latitudes where the motion of the spacecraft has a component toward the receiver, the shift without an ionosphere is greater than with an ionosphere because the ionospheric refraction acts to make the wave normal less nearly parallel to the spacecraft velocity vector than in the free-space case resulting in a lower positive shift. The difference goes positive for algebraicly similar reasons on the southern half of the pass. Reversing the direction of satellite motion would result in a difference curve that is reflected about the latitude axis. At the extremities of the curves, the difference value tends to come back to zero. The reflection cutoff at the southern end of the passes occurs at a lower latitude on the east pass because the inclination of the satellite orbital trajectory is such as to allow the satellite to move farther south before the great-circle distance reaches the cutoff value.

To obtain an estimate of the systematic east-west gradient, Ottawa ground ionosonde values of foF2 were plotted as a function of local time using data from the first half of January 1976. The OSCAR-6 local solar time was about 09 hr for the three southbound passes studied. The ionosonde data implied that eastward plasma frequency gradients of the order of 1 kHz/km existed in the ionosphere at 09 hr. Occasionally westward gradients of the same order of magnitude occured. Accordingly, the east-west gradient was set at plus and minus 0.001 MHz/km corresponding to the solid and broken curves respectively in Figure 2. For the 'East' pass, the amplitude of the ionospheric Doppler difference curve increases as the horizontal gradient changes from east to west. For the 'Overhead' pass there is no important dependence on the direction of the horizontal gradient. For the 'West' pass, the amplitude of the difference curve decreases as the gradient changes from east to west. The constant gradient experienced by the ray has the effect of bending the wave-normal directions away from the direction of the horizontal gradient. Otherwise there is no dramatic change from the no-gradient case.

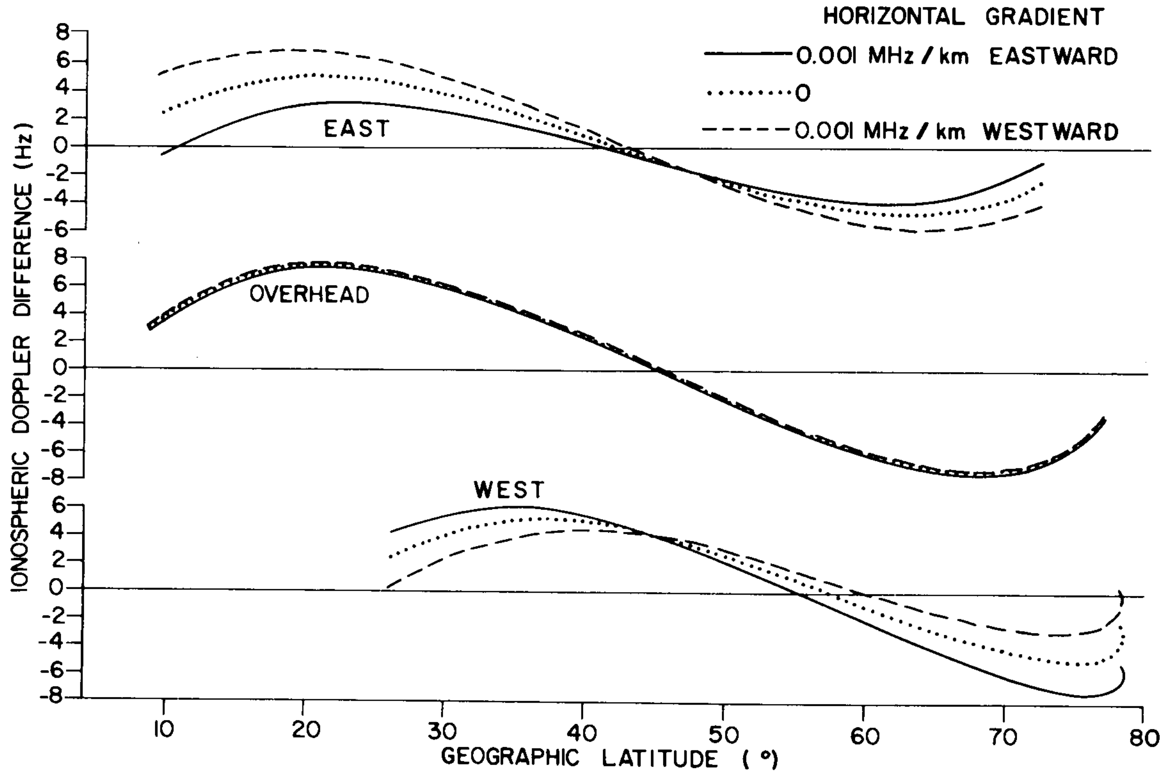

Figure 2. Ionospheric Doppler difference as a function of geographic latitude for three OSCAR-6 passes. Cases with no horizontal gradient in foF2, with an eastward gradient in foF2, and with a westward foF2 gradient are presented.

3.2.2 Figure 3

The use of unsmoothed topside sounder data to model the north-south density distribution results in a more irregular Doppler curve. At the bottom of Figure 3 is the latitudinal profile of foF2 exhibiting strong southward gradients near Ottawa but a rather flatter distribution to the north and south. The Figure illustrates that a ray crosses a region of the ionosphere at a latitude intermediate between the receiver and the satellite. The result is that the large excursions of the Doppler difference are displaced in latitude with respect to the fluctuations in the foF2 profile that caused them. The letters spaced along the profile and the "West" difference curve just above it indicate the realtionship. For instance, the "A" ray transmitted by OSCAR-6 at 25.5° latitude crosses the 350 km height in the ionosphere at a latitude of 34° and a positive Doppler difference of 4.8 Hz is calculated. The sharp positive peaks in the Doppler curve at A,E and I are seen to be caused by large southward density gradients.

In all the sets of curves, it is seen that the variations on the overhead Doppler curve are smaller than on the other two passes. This is due to the fact that the ray has a longer ionospheric path under the influence of the gradients on the oblique paths to the east or west orbits than it does on overhead paths.

3.2.3 Figure 4

The ISIS II sounder data reduce to a latitudinal profile of foF2 which has a modest southward gradient north of Ottawa and a reasonably deep depression to the south as plotted at the bottom of Figure 4. The comparatively large negative excursion of the Doppler difference around 35° latitude arises from the refractive effects of the depression. The displacement in latitude of the Doppler excursion with respect to the depression due to the obliquity of rays is again observed.

3.2.4 Figures 5a, 5b, 5c

The implementation of a deep trough in the foF2 profile centred at Ottawa has a dramatic effect on the Doppler difference frequency. The overhead pass in Figure 5b is plotted over the density profile, and the pairs of letters on the two curves show again that the largest effects correspond to rays that experience the largest north-south gradients while passing through the ionospheric layer. The depth of the trough (5 MHz) is representative of some of the deeper troughs observed by Muldrew (1965), and may be regarded as a typical upper limit. The total ionospheric Doppler difference of a few tens of hertz in Figures 5a and 5c is about as large as will ever be observed since the deep depression of foF2 was positioned at the most influential latitude: that of the receiver.

3.2.5 Figure 6

In the final example, a constant eastward gradient of 0.5 kHz/km was combined with foF2 and its southward gradient derived from the ISIS data profile at the bottom of the Figure 6. This leads to the solid curve in Figure 6. The central portion of the foF2 profile that acts on the Doppler curve is free of long scale systematic gradients but has small variations in foF2 which cause latitudinal fluctuations in the Doppler difference near Ottawa. The broken line was obtained by using the foF2 profile for the plasma frequency and setting all gradients to zero. Again, the results reveal that the small-scale gradients lead to differences of the order of a few hertz.

4. CONCLUDING REMARKS

Ionospheric refraction will typically cause systematic and random errors of a few hertz at 30 MHz if no horizontal gradients are assumed between an ELT and SARSAT and between SARSAT and Ottawa. Large density gradients including troughs, can exist in the F region and these will be responsible for the largest errors. Magnetically disturbed conditions occur occasionally and the main trough can then be centred near Ottawa; for the OSCAR-6 case errors of a few tens of hertz could result. For normal magnetic conditions, the main trough is north of Ottawa and errors of about 10 Hz for the OSCAR-6 case occur.

The plasma-frequency profile presented in Figure 6 applies to a local time of 0830 hrs. Irregularities in plasma frequency f_N and north-south variations in this figure are fairly typical for morning and early afternoon conditions; the magnitude of f_N, however, will vary throughout the day. The

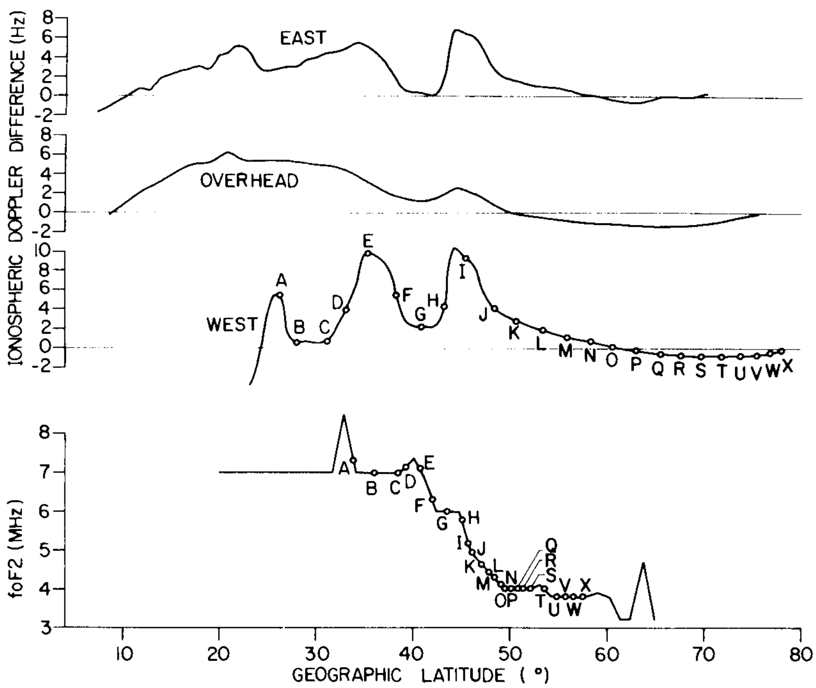

Figure 3. Ionospheric Doppler difference curves for three OSCAR-6 passes and obtained from ISIS-II data as a function of geographic latitude.

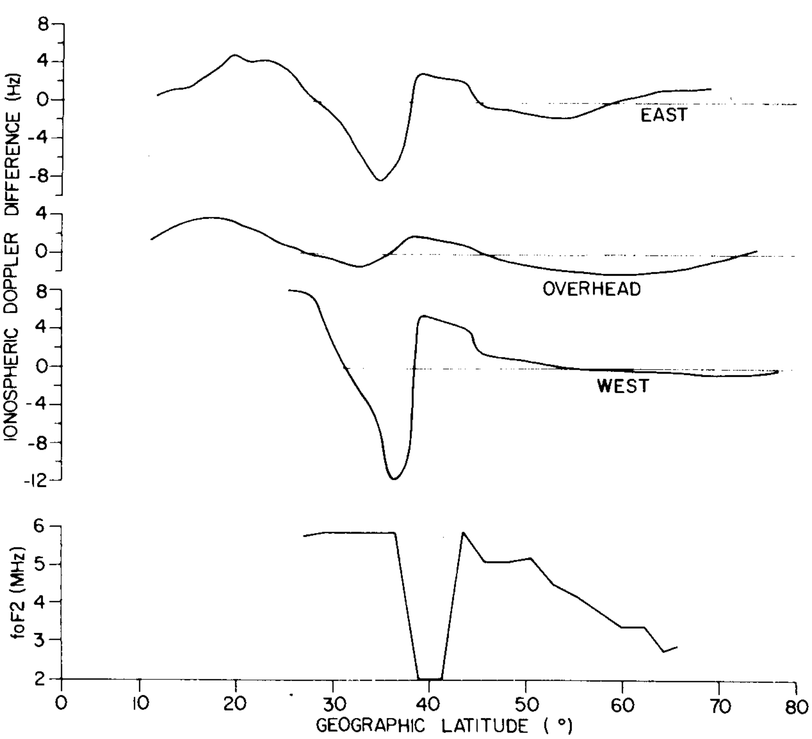

Figure 4. Ionospheric Doppler difference curves for three OSCAR-6 passes and obtained from ISIS-II data as a function of geographic latitude.

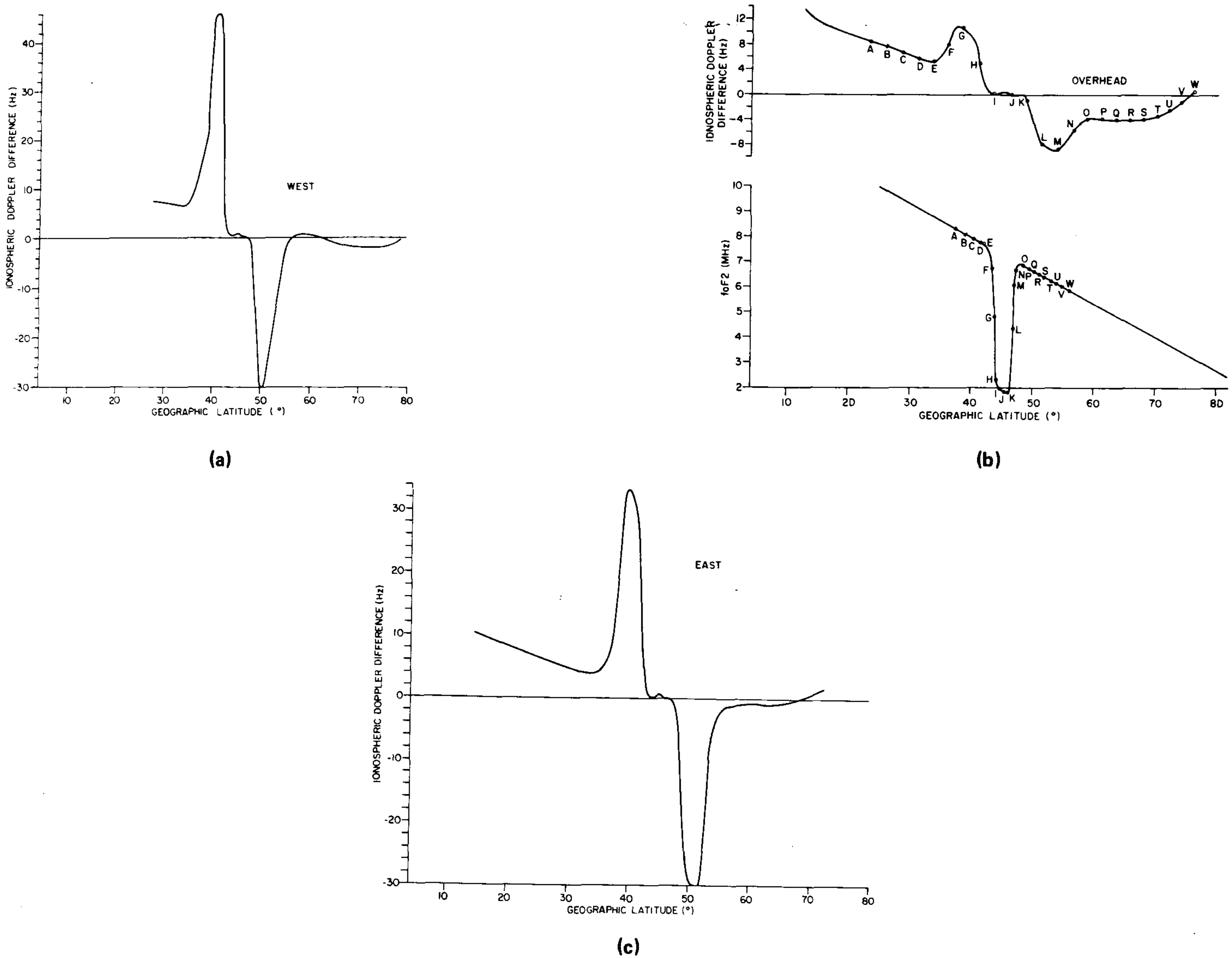

Figure 5. Ionospheric Doppler difference as a function of geographic latitude for three OSCAR-6 passes and hypothetical foF2 distribution as a function of geographic latitude.

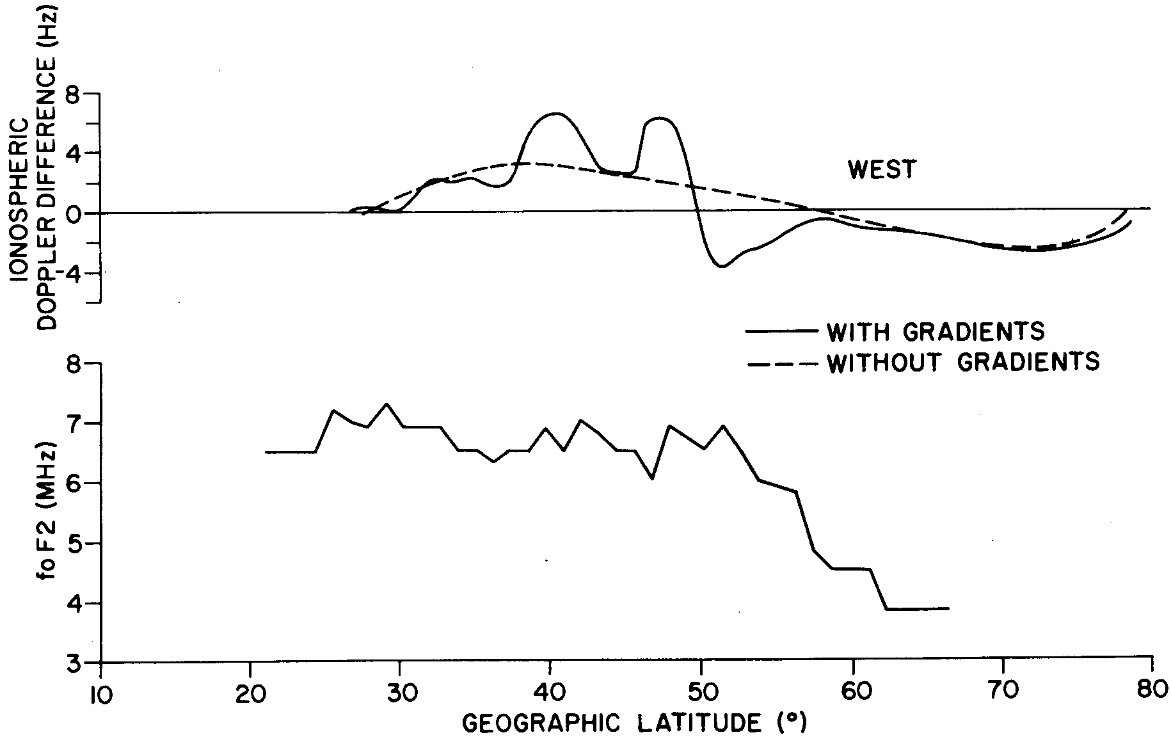

Figure 6. Ionospheric Doppler difference curves for three OSCAR-6 passes and obtained from ISIS-II data as a function of geographic latitude. The solid curve includes the effects of both the north-south and east-west gradients. The broken curve corresponds to the no-horizontal-gradient case.

main trough (Muldrew, 1965) is a regular feature of the ionosphere. It begins to form about 1500 hrs local time and becomes very pronounced from about 1700-2100 hrs. Between 2100 hrs and sunrise it is still present but is not so well defined. In the afternoon it moves southward and from about 1800 hrs to sunrise during normal magnetic activity it is located near 60° geomagnetic latitude or about 49° geographic latitude at the Ottawa longitude. During the night other troughs or rapid variations in f_N with latitude can occur throughout the high-latitude ionosphere.

In order to use these programs effectively for real-time ionospheric correction in the SARSAT system, a model of the required ionospheric parameters for North America would be required. This model would give critical F-layer frequencies and horizontal electron-density gradients, and perhaps effective F-layer thickness, as a function of longitude, latitude, local time, month, sunspot number and magnetic-activity index (Kp). It is hoped that such a model will be completed by mid 1978.

Doppler difference curves have been calculated at other frequencies than 30 MHz. The conditions corresponding to the solid curve in Figure 6 were applied to frequencies of 121.5, 143 and 406 MHz which are of interest in a SARSAT system. The shapes of the resulting difference curves remained unchanged but their amplitudes were lower by a factor of approximately the inverse ratio of the frequencies. For instance, the solid 30-MHz curve in Figure 6 has a peak at 47° latitude of about 6.3 Hz, whereas the calculated 121.5-MHz maximum at that latitude is 1.3 Hz.

5. REFERENCES

1. Lambert, J.D., and A.E. Winter, *A Search and Rescue Satellite System (SARSAT) Experiment*, IEEE Conference Publication 139, 351-355, 1976.

2. Muldrew, D.B., *F-Layer Ionization Troughs Deduced from Alouette Data*, J. Geophys. Res., 70, 2635, 1965.

3. Story, L.R.O., *A Method to Interpret the Dispersion Curves of Whistlers*, R.P.L. Report 23-4-1, p. 33, Defence Research Telecommunications Establishment, Ottawa, Canada, 1958.

APPENDIX I

CALCULATION OF THE DOPPLER FREQUENCY

APPENDIX I

Calculation of the Doppler Frequency

I.1 NO-IONOSPHERE CASE

The geometry for the no-ionosphere case is shown in Figure I.1 where the propagation is in a straight line from the ground station, assumed to be Ottawa (45.36°, -75.88°), to the satellite at height h_s above the earth's surface. The earth is assumed to be spherical with radius R = 6371 km. The angle subtended at the centre of the earth by the ground station and satellite is Θ and Φ is the angle of incidence of the ray at the satellite.

The latitude θ_s, longitude ϕ_s and height of the satellite are obtained using orbit calculation programs and data supplied by NASA; the latitude θ_o and longitude ϕ_o of the station are given. For a right-handed, rectangular coordinate system (x',y',z') fixed in the earth with origin at the earth's center, z' axis intersecting the north geographic pole and x' axis intersecting 0° latitude, 0° longitude (0°,0°), the satellite position is

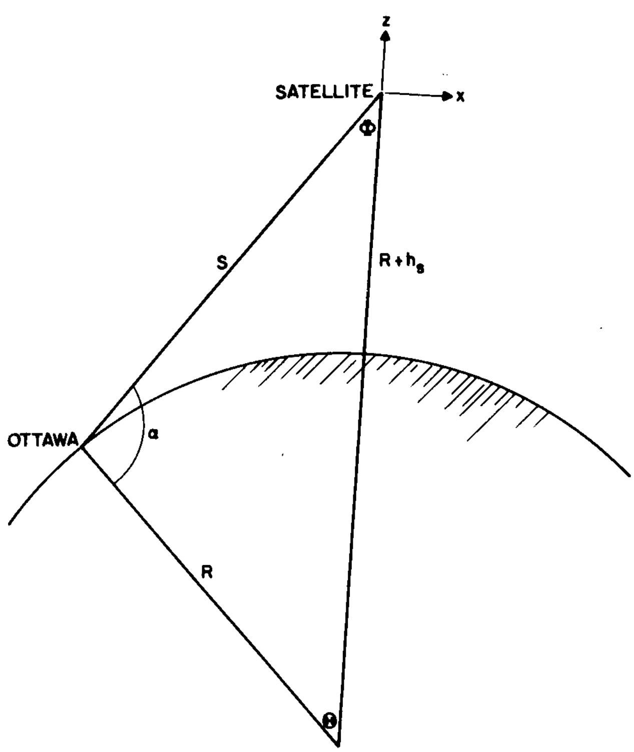

Figure I.1. Geometry for no-ionosphere case

$$\underline{P}_s = (R + h_s)\ (\underline{i}' \cos\theta_s \cos\phi_s + \underline{j}' \cos\theta_s \sin\phi_s + \underline{k}_1' \sin\theta_s) \qquad (I.1.1)$$

Unit vectors in the x', y' and z' direction are $\underline{i}'$, $\underline{j}'$ and $\underline{k}_1'$; the subscript 1 on $\underline{k}_1'$ is to distinguish this unit vector from the wave normal $\underline{k}'$ which will be defined later. The position of the ground station is

$$\underline{P}_o = R(\underline{i}' \cos\theta_o \cos\phi_o + \underline{j}' \cos\theta_o \sin\phi_o + \underline{k}_1' \sin\theta_o) \qquad (I.1.2)$$

Hence from $(\underline{P}_o \cdot \underline{P}_s)/|P_o P_s|$

$$\Theta = \cos^{-1}[\cos\theta_s \cos\theta_o \cos(\phi_s - \phi_o) + \sin\theta_s \sin\theta_o] \qquad (I.1.3)$$

where Θ is chosen so that $0° \leq \Theta \leq \pi$

From Figure I.1, the distance S between the satellite and fixed station is given by

$$S^2 = R^2 + (R + h_s)^2 - 2R\ (R + h) \cos\Theta \qquad (I.1.4)$$

and hence Φ is obtained from

$$\sin\Phi = R \sin\Theta/S \qquad (I.1.5)$$

If $\alpha = \pi - \Phi - \Theta < \frac{\pi}{2}$, then the satellite is out of range of the station.

Equation 1.1 can be written

$$f_D = -\frac{1}{2\pi}(k_x V_x + k_y V_y + k_z V_z) \qquad (I.1.6)$$

where

$$\underline{k} = \underline{i}\, k_x + \underline{j}\, k_y + \underline{k}_1\, k_z \qquad (I.1.7)$$

and

$$\underline{V} = \underline{i}\, V_x + \underline{j}\, V_y + \underline{k}_1\, V_z \qquad (I.1.8)$$

The z axis is the vertical through the satellite and the x axis is in the horizontal plane and is directed away from the fixed station. The (x, y, z) coordinate system at any instant is assumed fixed with respect to the earth. Hence

$$f_D = -\frac{f}{c}(V_x \sin\Phi + V_z \cos\Phi) \qquad (I.1.9)$$

where f is the transmitter frequency and c is the free space velocity of light.

I.2 SATELLITE VELOCITY

To check the accuracy of the calculations in the fixed-earth system using (I.1.6), the Doppler was calculated independently using celestial coordinates. In one case, it was found that errors of about 0.1° in specifying the latitude and/or longitude of the fixed station resulted in errors of up to about one hertz. Also, the satellite velocity was required to be defined carefully. Calculating the satellite velocity from two satellite positions one second apart and applying this to one of the positions rather than the average position could result in errors of about one hertz. The satellite velocity in (x,y,z) coordinates is calculated below.

Let the satellite position at a particular time be $\underline{P}_s$ and at T seconds later be $\underline{P}_{s1}$. $\underline{P}_{s1}$ can be obtained from (I.1.2) by changing the subscript s to s1. Then

$$\underline{V} = (\underline{P}_{s1} - \underline{P}_s)/T \qquad (I.2.1)$$

In (x',y',z') coordinates

$$V'_x = [(R + h_{s1}) \cos \theta_{s1} \cos \phi_{s1} - (R + h_s) \cos \theta_s \cos \phi_s]/T$$

$$V'_y = [(R + h_{s1}) \cos \theta_{s1} \sin \phi_{s1} - (R + h_s) \cos \theta_s \sin \phi_s]/T \qquad (I.2.2)$$

$$V'_z = [(R + h_{s1}) \sin \theta_{s1} - (R + h_s) \sin \theta_s]/T$$

To obtain $\underline{V}$ in (x,y,z) coordinates, it can be seen from Figure I.2 that

$$\underline{V} = V\,[\underline{i} \sin \alpha_2 \sin \alpha_3 + \underline{j} \sin \alpha_2 \cos \alpha_3 + \underline{k}_1 \cos \alpha_2] \qquad (I.2.3)$$

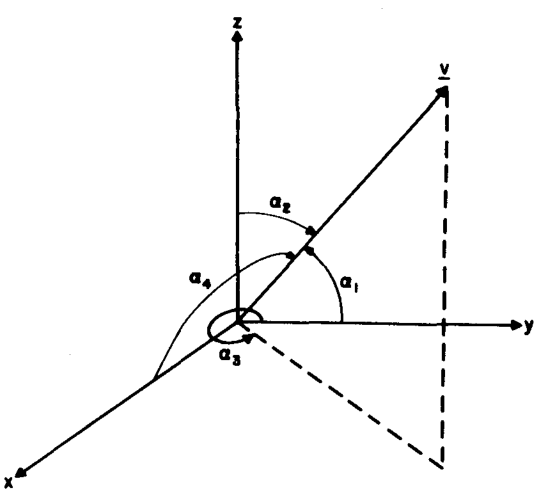

Figure I.2. Direction cosines of satellite velocity vector

The angle α_2 between $\underline{V}$ and the z axis is given by

$$\cos \alpha_2 = \frac{\underline{V} \cdot (\underline{P}_s + \underline{P}_{s1})}{|\underline{V}| \; |\underline{P}_s + \underline{P}_{s1}|} \tag{I.2.4}$$

where $\frac{1}{2} (\underline{P}_s + \underline{P}_{s1})$ is the average position of the satellite.

To obtain α_3 note that

$$V \cos \alpha_1 = V \sin \alpha_2 \cos \alpha_3 \tag{I.2.5}$$

and $\cos \alpha_1$ is given by

$$\cos \alpha_1 = \frac{\underline{V} \cdot \underline{j}}{|\underline{V}|} \tag{I.2.6}$$

$\underline{j}$ is perpendicular to the plane containing the position vector of the fixed station and the average position vector of the satellite.

$$\underline{j} = \frac{\underline{P}_o \times (\underline{P}_s + \underline{P}_{s1})}{|\underline{P}_o \times (\underline{P}_s + \underline{P}_{s1})|} \tag{I.2.7}$$

$$\underline{j} = \frac{\underline{i}' J_{x'} + \underline{j}' J_{y'} + \underline{k}_1' J_{z'}}{\left[J_{x'}^2 + J_{y'}^2 + J_{z'}^2\right]^{\frac{1}{2}}} \tag{I.2.8}$$

where

$$J_{x'} = \cos \theta_o \sin \phi_o \left[(R + h_s) \sin \theta_s + (R + h_{s1}) \sin \theta_{s1}\right]$$

$$- \sin \theta_o \left[(R + h_s) \cos \theta_s \sin \phi_s + (R + h_{s1}) \cos \theta_{s1} \sin \phi_{s1}\right]$$

$$J_{y'} = -\cos \theta_o \cos \phi_o \left[(R + h_s) \sin \theta_s + (R + h_{s1}) \sin \theta_{s1}\right] \tag{I.2.9}$$

$$+\sin \theta_o \left[(R + h_s) \cos \theta_s \cos \phi_s + (R + h_{s1}) \cos \theta_{s1} \cos \phi_{s1}\right]$$

$$J_{z'} = \cos \theta_o \cos \phi_o \left[(R + h_s) \cos \theta_s \sin \phi_s + (R + h_{s1}) \cos \theta_{s1} \sin \phi_{s1}\right]$$

$$- \cos \theta_o \sin \phi_o \left[(R + h_s) \cos \theta_s \cos \phi_s + (R + h_{s1}) \cos \theta_{s1} \cos \phi_{s1}\right]$$

It now appears that $\underline{V}$ in (x,y,z) coordinates can be obtained from(I.2.3) but there is insufficient information above to obtain the sign of sin α_3. To accomplish this cos α_4 is obtained from

$$\cos \alpha_4 = \frac{\underline{V} \cdot \underline{i}}{|\underline{V}|} = \frac{\underline{V} \cdot (\underline{j} \times \underline{k}_1)}{|\underline{V}|} \tag{I.2.10}$$

where $\underline{j}$ is given by (I.2.9) and $\underline{k}_1$ is

$$\underline{k}_1 = \frac{(\underline{P}_s + \underline{P}_{s1})}{|\underline{P}_s + \underline{P}_{s1}|} \tag{I.2.11}$$

and

$$\sin \alpha_3 = [1 - \cos^2 \alpha_3]^{\frac{1}{2}} \frac{\cos \alpha_4}{|\cos \alpha_4|} \tag{I.2.12}$$

I.3 IONOSPHERE, NO HORIZONTAL GRADIENTS

For curved earth and an ionosphere composed of a spherically stratified thick layer, Snell's law can be stated

$$n(R + h) \sin \Phi = \text{CONST} \tag{I.3.1}$$

where n and Φ are respectively the refractive index and angle between the wave normal and the vertical at distance R+h from the centre of the earth. The refractive index above and below the layer is 1 and in the layer

$$n = n_o = [1 - f_N^2/f^2]^{\frac{1}{2}} \tag{I.3.2}$$

where f_N is the plasma frequency or critical frequency (foF2) of the slab and f is the ray frequency.

As illustrated in Figure I.3 the ionosphere is approximated by a spherically thick layer with a constant plasma frequency between 200 and 500 km. The use of a more sophisticated model at the present time is not justified since any predicted value of f_N would not be sufficiently accurate. The 200 and 500 km values are based on experience from bottomside and topside ionograms. If a model ionosphere is capable of predicting better values for h_1 and h_2, the program can easily be changed to accomodate these values.

From Figure I.3 and (I.3.1)

$$\begin{aligned} R \sin \Phi_1 &= (R + h_1) \sin \Phi_2 = n_o (R + h_1) \sin \Phi_3 = n_o (R + h_2) \sin \Phi_4 \\ &= (R + h_2) \sin \Phi_5 = (R + h_s) \sin \Phi' \end{aligned} \tag{I.3.3}$$

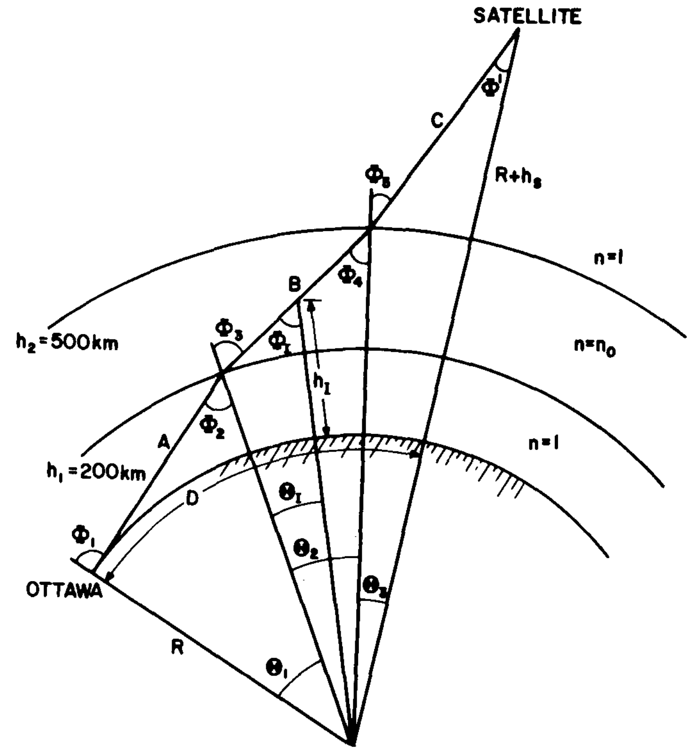

Figure I.3. Geometry for ionosphere case with no horizontal gradients

$$\Theta = \Theta_1 + \Theta_2 + \Theta_3 = (\Phi_1 - \Phi_2) + (\Phi_3 - \Phi_4) + (\Phi_5 - \Phi')$$

$$\begin{aligned} &= \left[\sin^{-1}\left(\frac{R + h_s}{R} \sin \Phi'\right) - \sin^{-1}\left(\frac{R + h_s}{R + h_1} \sin \Phi'\right)\right] \\ &+ \left[\sin^{-1}\left(\frac{R + h_s}{R + h_1} \frac{\sin \Phi'}{n_o}\right) - \sin^{-1}\left(\frac{R + h_s}{R + h_2} \frac{\sin \Phi'}{n_o}\right)\right] \\ &+ \left[\sin^{-1}\left(\frac{R + h_s}{R + h_2} \sin \Phi'\right) - \Phi'\right] \end{aligned} \tag{I.3.4}$$

To solve this implicit equation for Φ' by iteration, define

$$\begin{aligned} F \equiv - \Theta &+ \left[\sin^{-1}\left(\frac{R + h_s}{R} \sin \Phi'\right) - \sin^{-1}\left(\frac{R + h_s}{R + h_1} \sin \Phi'\right)\right] \\ &+ \left[\sin^{-1}\left(\frac{R + h_s}{R + h_1} \frac{\sin \Phi'}{n_o}\right) - \sin^{-1}\left(\frac{R + h_s}{R + h_2} \frac{\sin \Phi'}{n_o}\right)\right] \\ &+ \left[\sin^{-1}\left(\frac{R + h_s}{R + h_2} \sin \Phi'\right) - \sin^{-1}\left(\sin \Phi'\right)\right] \end{aligned} \tag{I.3.5}$$

Then, using Newton's method

$$\frac{\partial F}{\partial(\sin \Phi')} = \left[\frac{(R + h_s)/R}{\left[1 - \left(\frac{R + h_s}{R} \sin \Phi'\right)^2\right]^{\frac{1}{2}}} - \frac{(R + h_s)/(R + h_1)}{\left[1 - \left(\frac{R + h_s}{R + h_1} \sin \Phi'\right)^2\right]^{\frac{1}{2}}}\right] + \left[\quad\right] + \left[\quad\right] \tag{I.3.6}$$

Initially a value of $\sin \Phi'$ is guessed and the values of F and $\partial F/\partial(\sin \Phi')$ are calculated. Θ is obtained from (I.1.3). An improved value of $\sin \Phi'$ is obtained from

$$\sin \Phi' - F/\left[\frac{\partial F}{\partial(\sin \Phi')}\right]$$

Using this improved value, F and $\partial F/\partial(\sin \Phi')$ are again calculated and the process repeated until $\sin \Phi'$ is obtained to the desired accuracy. Φ_1 can be obtained from (I.3.4) and must be less than $\pi/2$ for the satellite to be in range.

The wave vector at the satellite is then given by

$$\underline{k} = \underline{i}\, k \sin \Phi' + \underline{k}_1\, k \cos \Phi' \tag{I.3.7}$$

and the Doppler frequency with no horizontal gradients is

$$f_{DI} = -\frac{f}{c}\left(V_x \sin \Phi' + V_z \cos \Phi'\right) \tag{I.3.8}$$

The Doppler obtained from (I.3.8) was verified using the alternate equation

$$f_{DI} = -\frac{f}{c}\frac{d}{dt}\int n\, ds \tag{I.3.9}$$

where ds is an incremental length along the ray path which, in this case, is the 3 lines A, B and C (Figure I.3).

1.4 IONOSPHERE WITH HORIZONTAL GRADIENTS

To calculate the effect of horizontal gradients, it is now assumed that the ray in the no-horizontal-gradient case is a straight line from the station to the satellite. The deviation of the path from this straight line due to the horizontal gradient will then be calculated and this deviation applied, at the satellite, to the actual no-horizontal-gradient case illustrated in Figure I.3 where the ray consists of 3 straight line sections.

If there is a horizontal gradient of electron density in the ionosphere, the portion of the ray in the ionosphere (see Figure I.3) will not be a straight line but will be curved away from the direction of the gradient. Note that the refraction due to the vertical gradient at h_1 in Figure I.3 is almost completely compensated at h_2 (cf. light passing through a pane of glass). This compensation does not occur with a horizontal gradient; hence a modest horizontal gradient can have a greater effect in total refraction on the ray than a large vertical gradient.

The radius of curvature R_c of the ray in the ionosphere, is given by another form of Snell's law [Storey, 1958]

$$\frac{1}{R_c} = -\frac{1}{n} (\nabla n)_\perp \tag{I.4.1}$$

where $(\nabla n)_\perp$ is the refractive index gradient perpendicular to the ray. The gradient ∇n is assumed constant between h_1 and h_2 and in the program is obtained by finding the average gradient along the ray between h_1 and h_2.

From (I.3.2), equation (I.4.1) can be written

$$\frac{1}{R_c} = \frac{1}{n_o^2} \frac{f_N}{f^2} (\nabla f_N)_\perp \tag{I.4.2}$$

Consider the (x", y", z") coordinate system with origin at the intersection of the ray with the height h_I of the layer centre. The z" axis is vertically upward and x" is in the vertical plane containing Ottawa and the satellite and is directed away from Ottawa. If ρ is the angle between the plasma frequency gradient ∇f_N and the y" axis, from Figure I.4

$$\nabla f_N = |\nabla f_N| \, [- \underline{i}'' \sin \rho + \underline{j}'' \cos \rho] \tag{I.4.3}$$

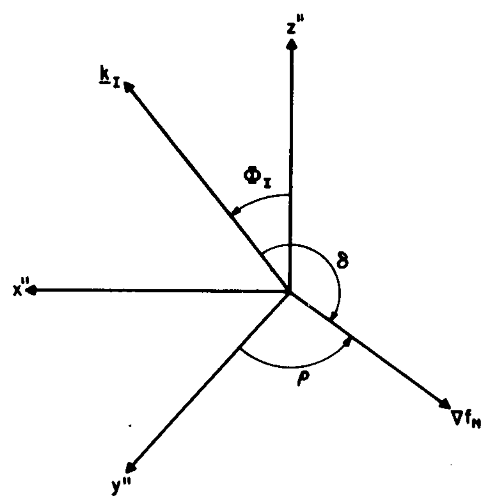

Figure I.4. Geometry at the midionosphere height h_I

Let the angle of incidence and the wave vector for the non-horizontal gradient case at height $h_I = (h_1 + h_2)/2$ be Φ_I and $\underline{k}_I$. The wave vector $\underline{k}_I$ is then

$$\underline{k}_I = k_I \left(\underline{i}'' \sin \Phi_I + \underline{k}_1'' \cos \Phi_I\right) \qquad \text{(I.4.4)}$$

If δ is the angle between $\underline{k}_I$ and ∇f_N, then the component of ∇f_N perpendicular to $\underline{k}_I$ in the plane containing $\underline{k}_I$ and ∇f_N is

$$(\nabla f_N)_\perp = |\nabla f_N| \sin \delta \qquad \text{(I.4.5)}$$

Taking the cross product of $\underline{k}_I$ and ∇f_N gives

$$\underline{\varepsilon}_1 (\nabla f_N)_\perp = |\nabla f_N| \left[\underline{i}'' \cos \Phi_I \cos \rho - \underline{j}'' \cos \Phi_I \sin \rho + \underline{k}_1'' \sin \Phi_I\right] \qquad \text{(I.4.6)}$$

where $\underline{\varepsilon}_1$ is a unit vector perpendicular to $\underline{k}_I$ and ∇f_N. Hence

$$(\nabla f_N)_\perp = \left[1 - \sin^2 \Phi_I \sin^2 \rho\right]^{\frac{1}{2}} |\nabla f_N| \qquad \text{(I.4.7)}$$

From (I.4.2)

$$\frac{1}{R_c} = \frac{1}{n^2} \frac{f_N}{f^2} \left[1 - \sin^2 \Phi_I \sin^2 \rho\right]^{\frac{1}{2}} |\nabla f_N| \qquad \text{(I.4.8)}$$

The deviation of the ray α, due to the horizontal gradient will now be determined.

The ray path looking vertically downward on the Ottawa-satellite path is shown in Figure I.5. The straight line OS is for no horizontal gradients. The path with horizontal gradients is broken into three parts, A below the slab, B in the slab, and C above the slab ionosphere. A and C are straight lines, B has radius of curvature R_c. α is very small so that to a good approximation the length of lines A, B and C can be obtained from Figure I.3 as

$$\begin{aligned} A &= R \sin \Theta_1 / \sin \Phi_1 \\ B &= (R + h_1) \sin \Theta_2 / \sin \Phi_4 \\ C &= (R + h_2) \sin \Theta_3 / \sin \Phi' \end{aligned} \qquad \text{(I.4.9)}$$

where Φ_1, Φ_4, Θ_1, Θ_2 and Θ_3 can be obtained in terms of Φ' from (I.3.3) and (I.3.4) and Φ' can be obtained by iteration as discussed above. From Figure I.3,

$$\sin \Phi_I = \frac{\left(R + h_s\right) \sin \Phi'}{n_o\left(R + h_I\right)} \qquad \text{(I.4.10)}$$

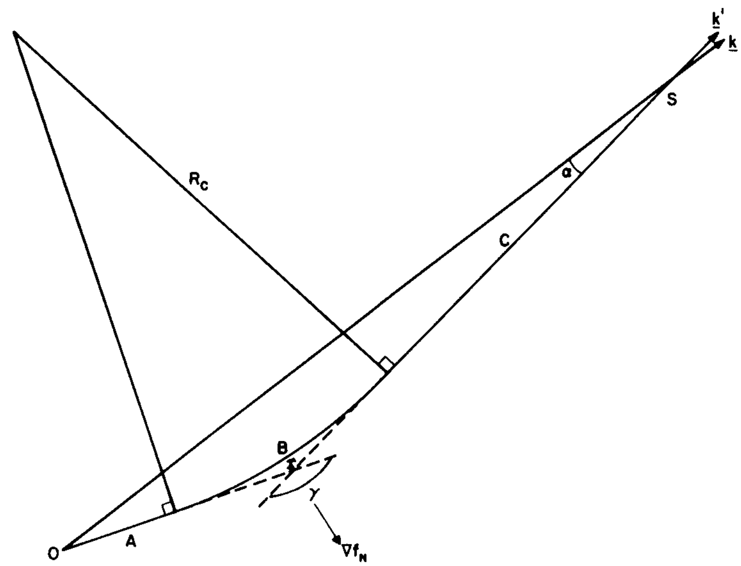

Figure I-5. Plan view of ray-path deviation due to a horizontal gradient

For the triangle OIS in Figure I.5,

$$\frac{\sin\alpha}{\overline{OI}} = \frac{\sin\alpha}{A + \frac{1}{2}B} = \frac{\sin\gamma}{A + B + C} \tag{I.4.11}$$

where

$$\gamma = \pi - B/R_c \tag{I.4.12}$$

In order to find the Doppler frequency it is necessary to determine $\underline{k}'$ the wave vector of the VHF wave modified by the ionosphere with horizontal gradients. $\underline{k}'$ can be obtained from α and the orientation of the plane containing the modified ray. The orientation of this plane is specified by μ, the angle between the vertical plane through Ottawa and the satellite and the plane containing the modified ray. The latter plane contains $\underline{k}$ (wave vector if no horizontal gradient) and $\underline{k}'$. Note that $\underline{k}$ is common to both planes and that ∇f_N is in the $(\underline{k}, \underline{k}')$ plane. The unit vector $\underline{\varepsilon}_1$ is then normal to the $(\underline{k}, \underline{k}')$ plane since it is being assumed that the ray in the no-horizontal-gradient case is a straight line. Note also that $\underline{j}''$ in the (x'', y'', z'') coordinate system with origin at height h_I is parallel, and hence equal, to $\underline{j}$ in the (x,y,z) coordinate system with origin at the satellite. $\underline{j}$ is normal to the vertical plane, hence from (I.4.5) and (I.4.6)

$$\cos\mu = \underline{\varepsilon}_1 \cdot \underline{j} = \underline{\varepsilon}_1 \cdot \underline{j}'' = -\cos\Phi_I \sin\rho/\sin\delta \tag{I.4.13}$$

μ and α are now known and $\underline{k}'$ in (x,y,z) coordinates remains to be determined.

In the (x,y,z) coordinate system at the satellite

$$\cos \mu = \varepsilon_o \left| \underline{j} \cdot \left(\frac{\underline{k}' \times \underline{k}}{k^2 \sin \alpha} \right) \right| \tag{I.4.14}$$

where $\varepsilon_o = \pm 1$ since at this point there is uncertainty in the sign of $\cos \mu$ and $|\underline{k}'| = |\underline{k}| = k$. From (I.3.7) and setting $\underline{k}' = \underline{i}\, k_x' + \underline{j}\, k_y' + \underline{k}_1\, k_z'$

$$\underline{k}' \times \underline{k} = (\underline{i}\, k_x' + \underline{j}\, k_y' + \underline{k}_1\, k_z') \times (\underline{i}\, k \sin \Phi' + \underline{k}_1\, k \cos \Phi')$$

$$|\underline{k}' \times \underline{k}|_y = k\, [- k_x' \cos \Phi' + k_z' \sin \Phi'] \tag{I.4.15}$$

From (I.4.14) and (I.4.15)

$$\varepsilon_o\, k\, |\cos \mu| \sin \alpha = - k_x' \cos \Phi' + k_z' \sin \Phi' \tag{I.4.16}$$

From the dot product of $\underline{k}$ and $\underline{k}'$

$$k^2 \cos \alpha = \underline{k} \cdot \underline{k}' = k_x'\, k \sin \Phi' + k_z'\, k \cos \Phi' \tag{I.4.17}$$

Multiplying (I.4.16) by $\sin \Phi'$ and (I.4.17) by $\cos \Phi'$ and adding gives

$$k_z' = k\, [\varepsilon_o\, |\cos \mu| \sin \alpha \sin \Phi' + \cos \alpha \cos \Phi'] \tag{I.4.18}$$

From (I.4.16)

$$k_x' = k\, [\cos \alpha \sin \Phi' - \varepsilon_o\, |\cos \mu| \sin \alpha \cos \Phi'] \tag{I.4.19}$$

Since $k'^2 = k_x'^2 + k_y'^2 + k_z'^2$, then from (I.4.18) and (I.4.19)

$$k_y' = \varepsilon_2\, k\, |\sin \mu \sin \alpha| \tag{I.4.20}$$

where $\varepsilon_2 = \pm 1$ since there is uncertainty in the sign of k_y' $\cdot$ $\underline{k}'$ is now determined in terms of μ, α, Φ', ε_o and ε_2.

To calculate μ from (I.4.13), Φ_I can be obtained from (I.4.10), δ can be obtained from (I.4.5) and (I.4.7) once ρ is known and ρ is determined as follows.

Suppose the east $(\nabla f_N)_E$ and south $(\nabla f_N)_S$ components of the plasma-frequency gradient are known. From Figure I.6, which shows the orientation of ∇f_N in the horizontal plane at height h_I

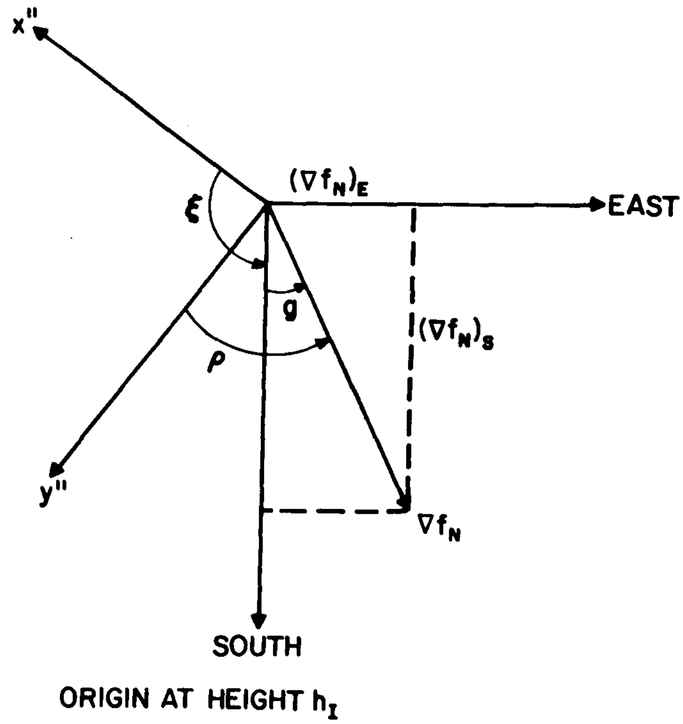

Figure I.6. Relationship of the (x'', y'', z'') coordinate system to the east and south directions

$$\rho = g + \xi - \frac{\pi}{2} \tag{I.4.21}$$

where

$$g = \tan^{-1} [(\nabla f_N)_E/(\nabla f_N)_S] \tag{I.4.22}$$

and ξ, the angle between south and the x'' axis at the height h_I is given by

$$\cos \xi = \frac{\underline{P}_o \times \underline{P}_I}{|\underline{P}_o \times \underline{P}_I|} \cdot \frac{\underline{P}_I(0,\phi_I) \times \underline{P}_I(\theta_I,\phi_I)}{|\underline{P}_I(0,\phi_I) \times \underline{P}_I(\theta_I,\phi_I)|} \tag{I.4.23}$$

Equation (I.4.23) states that ξ is the angle between the normal to the vertical plane through the station and the (x'', y'', z'') origin and the normal to the vertical plane directed south through the (x'', y'', z'') origin. The position vector $\underline{P}_o$ of the station in (x', y', z') coordinates is given by (I.1.2). The position vector $\underline{P}_I(\theta_I,\phi_I)$ of the (x'', y'', z'') origin must now be found in (x', y', z') coordinates. From Figure I.7

$$\underline{P}_I = r_3\, \underline{P}_o + r_4\, \underline{P}_s \tag{I.4.24}$$

where

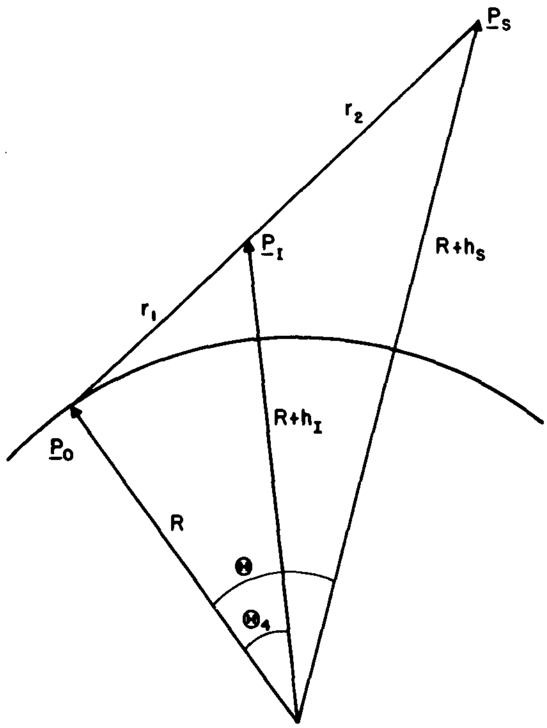

Figure I.7. Geometry for determining position vector $\underline{P}_I$

$$r_4 \equiv \frac{r_1}{r_1 + r_2} = \frac{\left(R + h_I\right) \sin \Theta_4}{\left(R + h_s\right) \sin \Theta} \tag{I.4.25}$$

and

$$r_3 \equiv \frac{r_2}{r_1 + r_2} = 1 - r_4 \tag{I.4.26}$$

Θ is given by (I.1.3) and $\Theta_4 = \Theta_1 + \Theta_I = \Theta_1 + (\Phi_3 - \Phi_I)$ from Figure I.3. Θ_1 is given by the first square bracket of (I.3.4), Φ_3 is given by the first term in the second square bracket of (I.3.4) and from (I.3.1) and Figure I.3, $\Phi_I = \sin^{-1} [(R + h_s)/(R + h_I) \cdot \sin \Phi'/n_o]$. If the latitude and longitude of the origin of the (x", y", z") coordinate system are (θ_I, ϕ_I) then

$$\begin{aligned}
(P_I)_{x'} &= \cos \theta_I \cos \phi_I = r_3 \cos \theta_o \cos \phi_o + r_4 \cos \theta_s \cos \phi_s \\
(P_I)_{y'} &= \cos \theta_I \sin \phi_I = r_3 \cos \theta_o \sin \phi_o + r_4 \cos \theta_s \sin \phi_s \qquad \text{(I.4.27)} \\
(P_I)_{z'} &= \sin \theta_I = r_3 \sin \theta_o + r_4 \sin \theta_s
\end{aligned}$$

and from (I.4.27)

$$\theta_I = \sin^{-1} [r_3 \sin \theta_o + r_4 \sin \theta_s]$$

$$\phi_I = \tan^{-1} [(r_3 \cos \theta_o \sin \phi_o + r_4 \cos \theta_s \sin \phi_s)/ (r_3 \cos \theta_o \cos \phi_o + r_4 \cos \theta_s \cos \phi_s)] \qquad (I.4.28)$$

Hence ρ can be calculated from (I.4.21), (I.4.22), (I.4.23), and (I.4.28).

Returning to the calculation of $\underline{k}'$, the values of α and Φ' can be obtained from (I.4.11) and from the iteration process. The signs ε_o and ε_2 are determined as follows.

Suppose $\mu = 90°$, then from (I.4.20)

$$k'_y = \varepsilon_2 k |\sin \alpha| \qquad (I.4.29)$$

Consider two positions of the satellite A and B as shown in Figure I.8. If ∇f_N has a component in the direction of y", then $k'_y < 0$ and vice versa. Hence

$$\varepsilon_2 = \frac{-\cos \rho}{|\cos \rho|} \qquad (I.4.30)$$

Suppose $\mu = 0°$ or $180°$ then the plane of the ray coincides with the vertical plane through Ottawa and the satellite. From (I.4.18) and (I.4.19)

$$k'_z = k \cos (\Phi' - \varepsilon_o |\alpha|)$$

and

$$k'_x = k \sin (\Phi' - \varepsilon_o |\alpha|) \qquad (I.4.31)$$

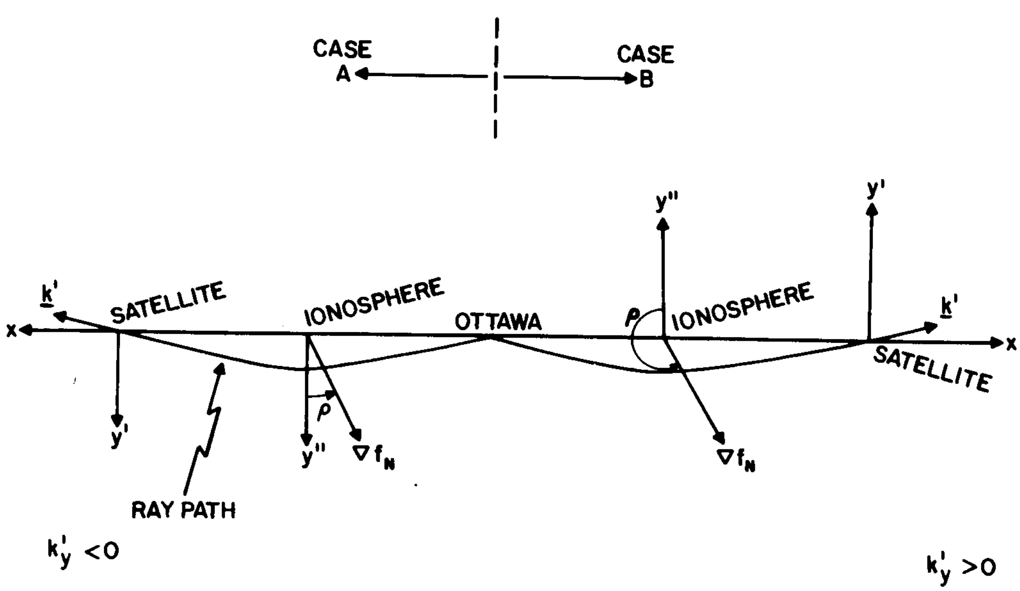

Figure I.8. Illustration to indicate how ε_2 can be obtained

If $\underline{k}$ has a component in the direction of ∇f_N, the refraction due to ∇f_N is such as to effectively decrease the value of Φ' so that $\varepsilon_o = +1$. Similarily if $\underline{k}$ has a component opposite in direction to ∇f_N, $\varepsilon_o = -1$. The component of $\underline{k}$ in direction ∇f_N is

$$\frac{\underline{k} \cdot \nabla f_N}{|\nabla f_N|} = k \cos \Phi' \frac{(\nabla f_N)_x}{|(\nabla f_N)|} \tag{I.4.32}$$

$\cos \Phi'$ is always positive so that

$$\varepsilon_o = (\nabla f_N)_x / |(\nabla f_N)_x| \tag{I.4.33}$$

From Figure I.6

$$(\nabla f_N)_x = |\nabla f_N| \cos (\xi + g) \tag{I.4.34}$$

Hence

$$\varepsilon_o = \cos (\xi + g)/|\cos (\xi + g)| \tag{I.4.35}$$

$\underline{k}'$ can now be calculated and hence the Doppler frequency with horizontal gradients is

$$\begin{aligned} f_{DIG} = -\frac{f}{c} [V_x & (\cos \alpha \sin \Phi' - \varepsilon_o |\cos \mu| \sin \alpha \cos \Phi') \\ & + V_y (\varepsilon_2 |\sin \alpha \sin \mu|) \\ & + V_z (\cos \alpha \cos \Phi' + \varepsilon_o |\cos \mu| \sin \alpha \sin \Phi')] \end{aligned} \tag{I.4.36}$$

APPENDIX II

PROGRAM OSCDOP5

```
C              PROGRAM OSCDOP5
C
C       OSCDOP5 CALCULATES THE EFFECT OF THE IONOSPHERE ON THE DOPPLER
C     FREQUENCY OF SARSAT SIGNALS.  BOTH VERTICAL AND HORIZONTAL ELECTRON
C     DENSITY GRADIENTS ARE CONSIDERED.  THE IONOSPHERE IS ASSUMED TO BE A
C     SPHERICAL SLAB OF CONSTANT DENSITY FROM 200  TO 500 KM HEIGHT.
C     !SET F:4/OSCAR6.284201C
C     !SET F:109/CALC3.284201C
C     !SET F:110/CALC2.284201G
C     !LINK BOSCDOP5,BINORB.284201Z,RVAN2B.284201G;SATT.:SYS;TSL.:SYS
C         BINORB DOES THE ORBITAL CALCULATIONS USING THE BROUWER MEAN
C     ORBITAL ELEMENTS IN OSCAR6.  CALC2 CONTAINS THE FOF2 VALUES
C     CORRESPONDING TO THE LATITUDES IN CALC3. RVAN2B IS FOR COORDINATE
C     TRANSFORMATIONS AND VECTOR OPERATIONS.
C     FOR OSCDOP4 AND ALL SUBROUTINES, INPUT AND OUTPUT LATS AND LONGS
C     ARE IN DEGREES.  ALL OTHER ANGLES ARE IN RADIANS.
        DIMENSION V1(3),V2(3),V3(3),V4(3),V5(3),V6(3)
        COMMON/COMFN/RLAT(500),FOF2(500),NR
C       READ IN LATS AND CORESPONDING FOF2  VALUES. LATS AND FOF2
C     VALUES ARE FROM RECORD #NSTART TO #NEND IN CALC2 AND CALC3.
 14     WRITE(108,98)
 98     FORMAT(1H1)
        WRITE(108,89)
  89    FORMAT(33H READ IN 0.(OR 1.) TO STOP(OR GO))
        READ(105,4) STOPGEN;IF(STOPGEN<1.) STOP
        WRITE(108,77)
 77     FORMAT(65H READ FNO,F15.5. FN OBTAINED FROM CALC2 AND CALC3 IF
       1FN=0.          )
        READ(105,4)FNO
        WRITE(105,78)
 78     FORMAT(18H READ DFNDSS,F15.5)
        READ(105,4)DFNDSS
        WRITE(108,99)
 99     FORMAT(18H READ DFNDSE,F15.5)
        READ(105,4)  DFNDSE
  4     FORMAT (F15.5)
        WRITE(108,93)
 93     FORMAT(26H READ NSTART AND NEND, 2I3)
        READ(105,500)NSTART,NEND
 500    FORMAT(2I3)
        NR=NEND-NSTART+1
        CALL POSREC(109,NSTART-1)
        CALL POSREC(110,NSTART-1)
        DO 501 J=1,NR
        READ(109,503)RLAT(J)
 501    READ(110,504)FOF2(J)
 503    FORMAT(20X,F6.2)
 504    FORMAT(13X,F2.0)
C       SAT POSITION CALCULATED 12 MIN BEFORE TO 12 MIN AFTER TIME
C     OF CLOSEST APPROACH.  LY=YEAR, LD=DAY, LH=HOUR, MIN=MINUTE
C     AND ISCA=SECOND OF CLOSEST APPROACH.  DOPPLER CALCULATIONS ARE
C     ISTEP SECONDS APART.
        PI=3.1415926536;P=PI/180.;R=6371.
```

```
         T1=45.36*P;P1=(360.-75.88)*P
         WRITE(108,94)
   94    FORMAT(22H READ LY AND LD, I2,I3)
         READ(105,1) LY,LD
         NSY=86400*LD
    1    FORMAT(I2,I3)
         LH=MIN=LS=LSTART=0
         CALL ORBITX(LY,LD,LH,MIN,LS,DLAT,DLONG,HGT,FFG,DIP
        C,LDIP,CHI,LSTART,4)
         WRITE(108,95)
   95    FORMAT(27H READ LH, MIN AND ISCA, 3I2)
         READ(105,2) LH,MIN,ISCA
         WRITE(108,96)
   96    FORMAT(15H READ ISTEP, I2)
         READ(105,2) ISTEP
    6    FORMAT(I4,I2)
    2    FORMAT(3I2)
         WRITE(108,91)
         WRITE(108,97)
   91    FORMAT(110H0YR DAY HR MN SEC  DLAT  DLONG    HGT     DIST     FN
        1 DFNDS     G    DOPC    DOPE    DOPI    DOPG  DDOPI  DDOPG       )
   97    FORMAT(110H0                    ( DEGREES)    (     KM     )    MHZ
        1 MHZ/KM DEGREES (        DOPPLER (HZ)                   )        )
         WRITE(108,92)
   92    FORMAT(X)
         MIN=MIN-12
   18    REPEAT 5,FOR LS=(ISCA,ISCA+1440,ISTEP)
         LS=LS+1
C          30-MHZ DOPPLER SHIFT WITHOUT IONOSPHERE  USING CELESTIAL COORDS
C          WHERE REL VELOC VECTOR IS V4 AND OTTAWA-SAT SEP VECTOR IS V5
         CALL ORBITX(LY,LD,LH,MIN,LS,DLAT,DLONG,HGT,FFG,DIP
        C,LDIP,CHI,LSTART,4)
         TS1=DLAT
         PS1=DLONG
         HS1=HGT
         T3=DLAT*P;P3=DLONG*P
         NSY=86400*LD+3600*LH+60*MIN+LS
         H=HGT+6371.
         CALL TRANSFORM(LY,H,0.,0.,T3,P3,NSY,V,TH3,PH3)
         CALL VCC(V,TH3/P,PH3/P,V3)
         CALL TRANSFORM(LY,6371.,0.,0.,T1,P1,NSY,V,TH4,PH4)
         CALL VCC(V,TH4/P,PH4/P,V6)
         LS=LS-1;NSY=NSY-1
         CALL ORBITX(LY,LD,LH,MIN,LS,DLAT,DLONG,HGT,FFG,DIP
        C,LDIP,CHI,LSTART,4)
         TS=DLAT
         PS=DLONG
         HS=HGT
         T2=DLAT*P;P2=DLONG*P
          H=HGT+6371.
```

```
         CALL TRANSFORM(LY,H,0.,0.,T2,P2,NSY,V,TH2,PH2)
         CALL VCC(V,TH2/P,PH2/P,V2)
         CALL TRANSFORM (LY,6371.,0.,0.,T1,P1,NSY,V,TH1,PH1)
         CALL VCC(V,TH1/P,PH1/P,V1)
         REPEAT 10, FOR I=1,2,3
         V4(I)=V3(I)-V2(I)-V6(I)+V1(I)
   10    V5(I)=((V2(I)-V1(I))+(V3(I)-V6(I)))/2.
         RELV=SQRT(V4(1)**2+V4(2)**2+V4(3)**2)
         FDG=-RELV*COS(ANGLE2(V4,V5)*P)/.01
C        CALCULATE AVERAGE FN, G AND DFNDSN OVER IONOSPHERIC PATH.
         HH=HHMIN=200.
         SUM1=SUM2=0.
         HHMAX=500.
         DO 20 II=1,100
         CALL IONCOOR(DLAT,DLONG,HH,HGT,TION,PION)
         CALL PLAS(TION,HH,FN,DFNDSN)
         SUM1=SUM1+FN
         SUM2=SUM2+DFNDSN
         HH=HH+25.
         IF(HH.GT.(HHMAX+0.1))GO TO 21
20       CONTINUE
21       FN=SUM1/II
         DFNDSN=SUM2/II
         IF (FNO.NE.0.)FN=FNO;DFNDSN=-DFNDSS
         DFNDSS=-DFNDSN
         IF(DFNDSE.EQ.0..AND.DFNDSS.EQ.0.)G=0.;GO TO 25
          G=ATAN(DFNDSE,DFNDSS)
25       GD=G/P
         H=HGT
          DFNDS=SQRT(DFNDSE**2+DFNDSS**2)
C      CALCULATE DOPPLER FREQUENCY IN EARTH COORDINATES.
         FD=FDI=FDIG=DFD=DFDG=0.
         CALL SATV(TS,PS,TS1,PS1,1.,HS,HS1,VX,VY,VZ,TH,PO,TO)
         DIST=R*TH
         CALL DOP3(PO,TO,PS,TS,VX,VY,VZ,TH,FN,DFNDS,G,H,FD,FDI,
        1FDIG,DFD,DFDG)
  5      WRITE(108,3)LY,LD,LH,MIN,LS,DLAT,DLONG,HGT,DIST,FN,DFNDS,GD,FDG
        1,FD,FDI,FDIG,DFD,DFDG
  3      FORMAT(I2,3I3,I5,F6.1,3F8.1,F7.1,F8.5,F6.0,4F7.1,2F6.1)
         GO TO 14
         END
C
         SUBROUTINE VCC(VM,T,P,V)
C         CALCULATES VECTOR V IN CELESTIAL COORDS USING ITS MODULUS VM,
C      CODECLINATION T AND RIGHT ASCENTION P.
         DIMENSION   V(3)
         CALL UVCC(T,P,V)
         DO 2 I=1,3
  2      V(I)=VM*V(I)
         RETURN
         END
```

```
C
      SUBROUTINE IONCOOR(DLAT,DLONG,H,H3,T3,P3)
C   CALCULATES LAT AND LONG OF INTERSECTION OF STRAIGHT
C   LINE BETWEEN OTTAWA AND OSCAR6 WITH HEIGHT H IN    IONOSPHERE.
C   (DLAT,DLONG)=SAT COORDS.
C   H= HEIGHT IN IONOSPHERE.
C   H3=SAT HEIGHT.
C   (T3,P3)=GEOG. COORDS OF SUB IONOSPHERE HEIGHT
      PI=3.1415926536; P=PI/180. ;R=6371.
      DLAT=DLAT*P
      DLONG=DLONG*P
      ST2=SIN(DLAT);CT2=COS(DLAT)
      SP2=SIN(DLONG);CP2=COS(DLONG)
      ST1=SIN(45.36*P);CT1=COS(45.36*P)
      SP1=SIN(-75.88*P);CP1=COS(-75.88*P)
      GAM=ACOS(CT1*CT2*COS(DLONG+P*75.88)+ST1*ST2)
      SG=SIN(GAM);CG=COS(GAM)
      Q=R/(R+H3)-CG
      EPS=ACOS(Q/SQRT(SG*SG+Q*Q))
      GAM3=PI-EPS-ASIN((R+H3)/(R+H)*SIN(EPS+GAM))
      SG3=SIN(GAM3)
      R4=(R+H)/(R+H3)*SG3/SG
      R3=1.-R4
      T3=ASIN(R3*ST1+R4*ST2)
      P3=ATAN((R3*CT1*SP1+R4*CT2*SP2),(R3*CT1*CP1+R4*CT2*CP2))
      P3=P3/P
      T3=T3/P
      DLAT=DLAT/P
      DLONG=DLONG/P
      RETURN
      END
C
      SUBROUTINE PLAS(DLAT,H,FN,GRAD)
C      DETERMINES PLASMA FREQUENCY AND GRADIENT FROM TABULATED VALUES
C   FOR A GIVEN LATITUDE.
      COMMON/COMFN/RLAT(500),FOF2(500),NR
      DO 10 J=2,NR
      IF(SIGN(1.,(RLAT(J)-DLAT)).EQ.SIGN(1.,(DLAT-RLAT(J-1)))) GO TO 15
   10 CONTINUE
      WRITE(108,1);STOP
   15 GRAD=(FOF2(J)-FOF2(J-1))/(RLAT(J)-RLAT(J-1))
      FN=FOF2(J-1)+GRAD*(DLAT-RLAT(J-1))
      FN=FN/10.
      GRAD=GRAD/(H+6371.)/0.17453293
      RETURN
    1 FORMAT(17H LAT NOT IN RANGE)
      END
C
```

```
      SUBROUTINE SATV(TS,PS,TS1,PS1,T,HS,HS1,VX,VY,VZ,TH,PO,TO)
C     GIVEN THE SAT POSITION AT THE TIME OF INTEREST AND AT
C     AN INCREMENTAL TIME T LATER,SATV CALCULATES SAT VEL IN XYZ COORDS,
C     TH = ANGLE BETWEEN SAT AND OTTAWA AT CENTRE OF EARTH.
      PI=3.1415926536; P=PI/180.; R=6371.
      RPH=R+HS; RPH1=R+HS1
      TO=45.36*P;PO=-75.88*P
      TS=TS*P; PS=PS*P; TS1=TS1*P; PS1=PS1*P
      VO=RPH/T; V1=RPH1/T
      CTO=COS(TO); STO=SIN(TO)
      CPO=COS(PO); SPO=SIN(PO)
      CTS=COS(TS); STS=SIN(TS)
      CTS1=COS(TS1); STS1=SIN(TS1)
      CPS=COS(PS);SPS=SIN(PS)
      CPS1=COS(PS1); SPS1 =SIN(PS1)
      VXP=V1*CTS1*CPS1-VO*CTS*CPS
      VYP=V1*CTS1*SPS1-VO*CTS*SPS
      VZP=V1*STS1-VO*STS
      V=SQRT(VXP*VXP+VYP*VYP+VZP*VZP)
      PSPS1X=RPH*(CTS*CPS)+RPH1*CTS1*CPS1
      PSPS1Y=RPH*CTS*SPS+RPH1*CTS1*SPS1
      PSPS1Z=RPH*STS+RPH1*STS1
      PSPS1=SQRT(PSPS1X*PSPS1X+PSPS1Y*PSPS1Y+PSPS1Z*PSPS1Z)
      XPK=PSPS1X/PSPS1
      YPK=PSPS1Y/PSPS1
      ZPK=PSPS1Z/PSPS1
      XPJ=CTO*SPO*PSPS1Z-STO*PSPS1Y
      YPJ=-CTO*CPO*PSPS1Z+STO*PSPS1X
      ZPJ=CTO*CPO*PSPS1Y-CTO*SPO*PSPS1X
      PJ=SQRT(XPJ*XPJ+YPJ*YPJ+ZPJ*ZPJ)
      XPJ=XPJ/PJ;YPJ=YPJ/PJ;ZPJ=ZPJ/PJ
      CA1=(VXP*XPJ+VYP*YPJ+VZP*ZPJ)/V
      CA2=(VXP*PSPS1X+VYP*PSPS1Y+VZP*PSPS1Z)/(V*PSPS1)
      SA2=SQRT(1.-CA2*CA2)
      CA3=CA1/SA2
      CA4=VXP*(YPJ*ZPK-ZPJ*YPK)+VYP*(-XPJ*ZPK+ZPJ*XPK)
     1+VZP*(XPJ*YPK-YPJ*XPK)
      SA3=SQRT(1-CA3*CA3)*CA4/ABS(CA4)
      VX=V*SA2*SA3
      VY=V*SA2*CA3
      VZ=V*CA2
      CTH=(CTO*CPO*PSPS1X+CTO*SPO*PSPS1Y+STO*PSPS1Z)/PSPS1
      TH=ACOS(CTH)
      TS=TS/P
      PS=PS/P
      TS1=TS1/P
      PS1=PS1/P
      PO=PO/P
      TO=TO/P
      RETURN
      END
C
```

```
      SUBROUTINE DOP3(PO,TO,PS,TS,VX,VY,VZ,TH,FN,DFNDS,G,H,
     1FD,FDI,FDIG,DFD,DFDG)
C     PRGM DOP3 CALCULATES THE DOPPLER EFFECT OF THE IONOSPHERE
C     ON SIGNALS TRANSMITTED FROM A SATELLITE. CURVED EARTH
C     AND A CURVED SLAB IONOSPHERE ARE ASSUMED.
      PI=3.1415926536
      PS=PS*PI/180.
      PO=PO*PI/180.
      P=PI/180.
      TS=TS*P
      TO=TO*P
      SPO=SIN(PO);CPO=COS(PO)
      STO=SIN(TO);CTO=COS(TO)
      STS=SIN(TS);CTS=COS(TS)
      SPS=SIN(PS);CPS=COS(PS)
      R=6371.
      FF=30.
      H1=200.
      H2=500.
      RPH=R+H
      RPH1=R+H1
      RPH2=R+H2
      SPP=R/RPH*.9999
C CALC OF DOPPLER WITH NO IONOSPHERE.
      S=SQRT(R*R+RPH*RPH-2.*R*RPH*COS(TH))
      SP=R/S*SIN(TH)
      ALP=PI-TH-ASIN(SP)
      PID2=PI/2.
      IF(ALP.LT.PID2)WRITE(108,11)
11    FORMAT(42H SATELLITE OUT OF RANGE WITHOUT IONOSPHERE)
      CP=SQRT(1.-SP*SP)
      FD=-FF/3.E05*1.E06*(VX*SP+VZ*CP)
C    CALC OF PHI PRIMED (ANGLE OF INCIDENCE AT SAT) AND DOPPLER
C    DUE TO VERTICAL VARIATION OF ELECTRON DENSITY.
      IZZ=0
      GN=SQRT(1.-FN*FN/(FF*FF))
      C1=RPH/R;C2=RPH/RPH1;C3=C2/GN;C4=RPH/RPH2;C5=C4/GN
1     D1=C1*SPP;D2=C2*SPP;D3=C3*SPP;D4=C4*SPP;D5=C5*SPP
      IF(D3.GT.1..OR.D1.GT.1.)SPP=SPP*.999;GO TO 1
      IF(D1.GT.1.)D1=.9999999
      IF(D3.GT.1.)D3=.9999999
      IF(D2.GT.1.)D2=.9999999
       IF(D4.GT.1.)D4=.9999999
       IF(D5.GT.1.)D5=.9999999
      IZZ=IZZ+1
      IF(IZZ.GT.100)GO TO 5
      F=-TH+ASIN(D1)-ASIN(D2)+ASIN(D3)-ASIN(D5)+ASIN(D4)-ASIN(SPP)
      DFDSP=C1/SQRT(1.-D1*D1)-C2/SQRT(1.-D2*D2)+C3/SQRT(1.-D3*D3)
     1-C5/SQRT(1.-D5*D5)+C4/SQRT(1.-D4*D4)-1./SQRT(1.-SPP*SPP)
```

```
      DSPDF=1./DFDSP
      SPP1=SPP
      SPP=SPP1-F*DSPDF
      IF(ABS((SPP-SPP1)/SPP).GT.1.E-06)GO TO 1
      PHI1=TH+ASIN(D2)-(ASIN(D3)-ASIN(D5))-(ASIN(D4)-ASIN(SPP))
      PD2=PI/2.
      IF(PHI1.GT.PD2)GO TO 4
      GO TO 6
 4    WRITE(108,7);RETURN
 5    WRITE(108,9);RETURN
 7    FORMAT(39H SATELLITE OUT OF RANGE WITH IONOSPHERE)
 9    FORMAT(74H TELEMETRY REFLECTED, ITERATION FAILED,OR SAT OUT OF RAN
     1GE WITH IONOSPHERE          )
 6    CPP=SQRT(1.-SPP*SPP)
      FDI=-FF/3.E05*1.E06*(SPP*VX+CPP*VZ)
C   CALC OF AL AND DOPPLER WITH HORIZONTAL
C   ELECTRON DENSITY GRADIENT PRESENT. AL IS THE
C   DEVIATION OF THE RAY DUE TO THE HORIZONTAL GRADIENT.
      PA=ASIN(C2*SPP)
      PB=ASIN(C5*SPP)
      PC=ASIN(SPP)
      EA=ASIN(C1*SPP)-PA
      EB=ASIN(C3*SPP)-PB
      EC=ASIN(C4*SPP)-PC
      DA=R*SIN(EA)/SIN(PA)
      DB=RPH1*SIN(EB)/SIN(PB)
      DC=RPH2*SIN(EC)/SIN(PC)
      SPI=RPH*SPP/(0.5*(RPH1+RPH2)*GN)
      CPI=SQRT(1.-SPI*SPI)
      HI=0.5*(H1+H2)
      TS=TS/P;PS=PS/P
      CALL IONCOOR(TS,PS,HI,H,THII,PHII)
      TS=TS*P;PS=PS*P
      THII=THII*P;PHII=PHII*P
      ST3=SIN(THII);CT3=COS(THII)
      CP3=COS(PHII);SP3=SIN(PHII)
      POXPIX=CTO*SPO*ST3-STO*CT3*SP3
      POXPIY=-CTO*CPO*ST3+STO*CT3*CP3
      POXPIZ=CTO*CP3*(CPO*SP3-SPO*CP3)
      POXPI=SQRT(POXPIX**2+POXPIY**2+POXPIZ**2)
      XI=PI-ACOS((SP3*POXPIX-CP3*POXPIY)/POXPI)
C     IF(PO.LT.-72.*P)OUTPUT THII,PHII,POXPIX,POXPIY,
C    1POXPIZ,POXPI,CTO,SPO,STO,CT3,SP3
      XI=ABS(XI)*(PO-PHII)/(ABS(PO-PHII))
      RO=XI+G-PI/2.
      RC=GN*GN*FF*FF/FN/DFNDS/SQRT(1.-(SPI*SIN(RO))**2)
      GAM=PI-DB/RC
      SAL=(DA+0.5*DB)*SIN(GAM)/(DA+DB+DC)
      CAL=SQRT(1.-SAL*SAL)
      SDEL=SQRT(1.-(SPI*SIN(RO))**2)
      CPP=COS(ASIN(SPP))
      CMU=-CPI*SIN(RO)/SDEL
```

```
      CMU=-CPI*SIN(RO)/SDEL
      SMU=SQRT(1.-CMU*CMU)
      EPS2=-SIGN(1.,COS(RO))
      EPS1=COS(XI+G)/ABS(COS(XI+G))
      CON=-1.E06*FF/3.E05
      FDIGX1=CON*VX*CAL*SPP
      FDIGX2=-CON*VX*EPS1*ABS(CMU)*SAL*CPP
      FDIGY=CON*VY*EPS2*ABS(SAL*SMU)
      FDIGZ1=CON*VZ*CAL*CPP
      FDIGZ2=CON*VZ*EPS1*ABS(CMU)*SAL*SPP
      FDIG=-1.E06*FF/3.E05*(VX*(CAL*SPP-EPS1*ABS(CMU)*SAL*CPP)+
     1VY*(EPS2*ABS(SAL*SMU))+VZ*(CAL*CPP+EPS1*ABS(CMU)*SAL*SPP))
C     OUTPUT
      DFD=FDI-FD
      DFDG=FDIG-FD
      RETURN
      END
```

THIS PAGE INTENTIONALLY LEFT BLANK

A P P E N D I X I I I

COMPUTATIONS

```
!SET F:4/OSCAR6.284201C

!SET F:109/CALC3.284201G

!SET F:110/CALC2.284201G

!LINK BOSCDOP5,BINORB.284201G,RVAN2B.284201G;SATT.:SYS;TSL.:SYS
     LINKING  BOSCDOP5
     LINKING  BINORB
     LINKING  RVAN2B
     LINKING  SATT
     LINKING  TSL
'P1' ASSOCIATED.
     LINKING  SYSTEM LIB

!S

 READ IN 0.(OR 1.) TO STOP(OR GO)
?1.
 READ FNO,F15.5. FN OBTAINED FROM CALC2 AND CALC3 IF    FN=0.
?0.
 READ DFNDSS,F15.5
?0.
 READ DFNDSE,F15.5
?.0005
 READ NSTART AND NEND, 2I3
?001040
 READ LY AND LD, I2,I3
?76006
 READ LH, MIN AND ISCA, 3I2
?163233
 READ ISTEP, I2
?50
 READ FREQUENCY IN MHZ, F15.5
?30.

 YR DAY HR MN SEC  DLAT  DLONG    HGT     DIST    FN    DFNDS     G    DOPC   DOPR   DOPI   DOPG  DDOPI  DDOPG

                   ( DEGREES)    (   KM    )      MHZ   MHZ/KM DEGREES (        DOPPLER (HZ)                   )

 SATELLITE OUT OF RANGE WITHOUT IONOSPHERE
 TELEMETRY REFLECTED, ITERATION FAILED,OR SAT OUT OF RANGE WITH IONOSPHERE
76  6 16 20   33  76.8    1.6  1461.6  4814.9   4.6  .00241   12.  515.1  515.1     .0     .0     .0     .0
 SATELLITE OUT OF RANGE WITHOUT IONOSPHERE
 TELEMETRY REFLECTED, ITERATION FAILED,OR SAT OUT OF RANGE WITH IONOSPHERE
76  6 16 20   83  77.8   -9.4  1461.8  4557.4   4.8  .00247   12.  508.3  508.3     .0     .0     .0     .0
 SATELLITE OUT OF RANGE WITHOUT IONOSPHERE
 TELEMETRY REFLECTED, ITERATION FAILED,OR SAT OUT OF RANGE WITH IONOSPHERE
76  6 16 20  133  78.4  -21.9  1461.9  4304.6   5.0  .00183   16.  499.4  499.4     .0     .0     .0     .0
 SATELLITE OUT OF RANGE WITHOUT IONOSPHERE
76  6 16 20  183  78.4  -35.0  1461.9  4057.5   5.2  .00193   15.  487.9  487.9  487.9  486.8     .0   -1.1
76  6 16 20  233  77.9  -47.6  1462.0  3817.0   5.4  .00278   10.  473.2  473.2  472.6  471.6    -.6   -1.6
76  6 16 20  283  76.8  -58.8  1462.1  3584.6   5.7  .00305    9.  454.7  454.7  453.4  452.7   -1.3   -2.0
76  6 16 20  333  75.4  -68.1  1462.4  3361.9   6.0  .00273   11.  431.7  431.7  429.7  429.4   -2.0   -2.4
76  6 16 20  383  73.7  -75.7  1462.8  3151.1   6.2  .00172   17.  403.6  403.6  401.2  400.9   -2.4   -2.7
76  6 16 20  433  71.8  -81.8  1463.3  2954.8   6.3  .00149   20.  369.5  369.5  367.0  366.9   -2.5   -2.7
76  6 16 20  483  69.7  -86.8  1463.8  2776.0   6.5  .00128   23.  329.0  329.0  326.5  326.4   -2.4   -2.5
76  6 16 20  533  67.6  -90.9  1464.5  2618.3   6.6  .00138   21.  281.4  281.4  279.2  279.3   -2.2   -2.1
76  6 16 20  583  65.3  -94.4  1465.2  2485.8   6.7  .00082   38.  226.6  226.6  224.8  224.6   -1.8   -2.0
76  6 16 20  633  63.0  -97.4  1465.9  2382.6   6.7  .00063   53.  165.2  165.2  163.8  163.5   -1.4   -1.6
76  6 16 20  683  60.6  -99.9  1466.5  2312.6   6.7  .00069  134.   98.1   98.1   97.3   96.4    -.8   -1.7
76  6 16 20  733  58.2 -102.1  1467.0  2278.9   6.7  .00053   71.   27.3   27.3   27.1   26.8    -.2    -.5
76  6 16 20  783  55.8 -104.1  1467.5  2283.2   6.7  .00180  164.  -44.6  -44.6  -44.3  -46.4     .3   -1.7
76  6 16 20  833  53.4 -105.9  1467.7  2325.4   6.6  .00285  170. -115.0 -115.0 -114.1 -117.4     .9   -2.4
76  6 16 20  883  50.9 -107.5  1467.8  2403.5   6.3  .00274  169. -181.3 -181.3 -180.1 -183.2    1.3   -1.9
76  6 16 20  933  48.4 -108.9  1467.7  2514.4   6.2  .00356    8. -241.7 -241.7 -240.0 -236.0    1.7    5.7
76  6 16 20  983  45.9 -110.3  1467.3  2653.9   6.5  .00050   90. -295.0 -295.0 -292.8 -292.8    2.2    2.2
76  6 16 20 1033  43.4 -111.5  1466.6  2817.9   6.5  .00052   72. -341.0 -341.0 -338.5 -338.2    2.5    2.8
76  6 16 20 1083  40.9 -112.7  1465.6  3002.3   6.7  .00213   14. -379.8 -379.8 -376.8 -373.6    2.9    6.2
76  6 16 20 1133  38.3 -113.7  1464.4  3203.5   6.9  .00064   51. -411.9 -411.9 -408.7 -407.8    3.2    4.1
76  6 16 20 1183  35.8 -114.8  1463.0  3418.4   6.7  .00065  130. -438.1 -438.1 -435.4 -435.7    2.8    2.5
76  6 16 20 1233  33.2 -115.8  1461.3  3644.5   6.7  .00098  149. -459.3 -459.3 -457.1 -458.0    2.2    1.3
76  6 16 20 1283  30.7 -116.7  1459.6  3879.6   6.6  .00115  154. -476.2 -476.2 -474.9 -476.0    1.3     .2
 SATELLITE OUT OF RANGE WITHOUT IONOSPHERE
76  6 16 20 1333  28.1 -117.6  1457.9  4122.2   6.4  .00051   79. -489.5 -489.5 -489.4 -488.7     .1     .8
 SATELLITE OUT OF RANGE WITHOUT IONOSPHERE
 TELEMETRY REFLECTED, ITERATION FAILED,OR SAT OUT OF RANGE WITH IONOSPHERE
76  6 16 20 1383  25.6 -118.5  1456.3  4370.9   6.5  .00129   23. -499.9 -499.9     .0     .0     .0     .0
 SATELLITE OUT OF RANGE WITHOUT IONOSPHERE
 TELEMETRY REFLECTED, ITERATION FAILED,OR SAT OUT OF RANGE WITH IONOSPHERE
76  6 16 20 1433  23.0 -119.3  1454.9  4624.6   6.8  .00101   30. -508.0 -508.0     .0     .0     .0     .0

 READ IN 0.(OR 1.) TO STOP(OR GO)
?0.
 *STOP* 0

 !
```

CRC DOCUMENT CONTROL DATA

1. **ORIGINATOR:** Department of Communications/Communications Research Centre

2. **DOCUMENT NO:** CRC Report No. 1313

3. **DOCUMENT DATE:** February 1978

4. **DOCUMENT TITLE:** Ionospheric Effects on the Doppler Frequency Shift in SARSAT Propagation

5. **AUTHOR(s):** D.B. Muldrew and H.G. James

6. **KEYWORDS:**
   (1) Doppler
   (2) SARSAT
   (3) Propagation

7. **SUBJECT CATEGORY (FIELD & GROUP: COSATI)**

   20 Physics

   20 14 Wave Propagation

8. **ABSTRACT:**

The Doppler frequency shift of signals propagating from an Emergency Locator Transmitter (ELT) on a downed aircraft up to a transponder on a search and rescue satellite (SARSAT) and down to a central station is affected by the ionosphere. In this report ionospheric effects are estimated for a proof-of-concept SARSAT experiment using the AMSAT OSCAR-6 satellite. In this case, the down link is at 30 MHz and the daytime ionosphere with no horizontal gradients in electron density can change the Doppler frequency by a few hertz. Horizontal gradients of electron density can have more effect on the Doppler frequency than the vertical distribution of density since the negative vertical density gradient in the topside ionosphere tends to compensate the Doppler effect due to the positive gradient in the bottomside. In the late afternoon, evening and nighttime, large east-west troughs in the density distribution exist which can produce shifts of a few tens of hertz at 30 MHz. The Doppler frequency shift due to the ionosphere varies approximately inversely as the frequency. The results obtained here can be applied to the definition of an operational SARSAT system.

9. **CITATION:**

Government of Canada Gouvernement du Canada